# Theory of the inverted-population cavity amplifier

G. L. Mander and R. Loudon
*Department of Physics, University of Essex, Colchester, Essex, CO4 3SQ, England*

T. J. Shepherd
*Royal Signals and Radar Establishment, Malvern, Worcestershire, WR14 3PS, England*
(Received 14 July 1989)

We calculate the input-output characteristics of an optical amplifier that consists of an inverted-population medium placed inside a high-$Q$ Fabry-Pérot cavity. Expressions are derived for the output second- and fourth-order spectral and temporal correlation functions, and more generally for the output characteristic functional, in terms of the corresponding input quantities. The photocount first and second factorial moments are obtained for both homodyne and direct detection of the amplifier input and output. The general results are applied to several cases of practical interest, including inputs that have coherent or chaotic coherence properties. Particular attention is paid to the effects of amplification on specific nonclassical varieties of input light. It is shown that a maximum of only twofold amplification is permitted if any squeezing present in the input is to survive as squeezing in the output light. Similarly, for the preservation of photon antibunching in amplification, we show, by consideration of a kind of free-space number-state input, that only small gains are allowed. The amplifier model treated here provides a detailed example of the limitations imposed by quantum mechanics on the minimum noise generated by a multimode linear amplifier. In particular, we show that minimum noise occurs in a cavity that is asymmetric with respect to mirror reflectivities, for which we derive the corresponding conditions. In addition, we demonstrate the ability of the amplifier to improve upon signal-to-noise ratio, otherwise limited by low detector quantum efficiency.

## I. INTRODUCTION

Optical amplifiers are of considerable current interest in view of their potential importance in all-optical repeaters, and for predetection amplification in optical communication systems. Theoretical treatments of the inverted-population optical amplifier date back to the early considerations of the feasibility of laser action. These treatments mainly used semiclassical methods, with the amplifier noise modeled as a stationary Gaussian process. However, more recent interest in the possible applications of nonclassical light has led to the development of fully quantum-mechanical theories that are capable of evaluating the effects of amplification on the desirable low-noise properties of nonclassical light. Quantum-mechanical amplification theory provides very general limits on the minimum amounts of noise that must be added by any practical optical amplifier. These limits have been very clearly presented by Caves,[1] who also reviews earlier work on amplifier theory.

Much of the work on quantum-mechanical amplifier theory is based on a model developed by Louisell and his collaborators.[2,3] They used a Heisenberg-picture approach to the linearized treatment of a single-mode amplifier or attenuator, in which the spatial propagation of an optical signal through the amplifying medium is replaced by a time-dependent growth in optical intensity. The model contains no provision for the effects of coupling the input and output fields to the amplifying medium itself. These various limitations prevent any calculation of the effects of amplification on the spectral properties and multitime correlation functions of the amplified light beam, or of the effects of integration times on the corresponding detected quantities. However, the simplicity of this model, and of equivalent theories produced by other authors, allows a wide range of interesting properties to be calculated, including the effects of amplification on signal-to-noise ratios, nonclassical properties such as squeezing and antibunching, and other photon statistical quantities.[4-7] There has also been some progress in improving the basic model to include input and output fields, and converting the amplifier to steady-state operation.[8]

The purpose of the present paper, some of whose results have been summarized previously,[9] is an improvement in the Louisell model to allow multimode input and output light beams. The main modification is the insertion of an optical cavity to contain the inverted-population atoms of the amplifying medium. With a cavity of sufficiently high $Q$, it is permissible to assume that only a single internal mode is significantly excited by an input beam that covers a limited but continuous range of external modes. The dynamics of the coupling between internal and external modes is treated by methods developed recently for cavity systems.[10,11] The plane cavity mirrors are assumed to be oriented perpendicular to the input light beam, and the optical system is treated as one-dimensional, with any transverse effects ignored. The improved model thus remains reasonably simple, and it is possible to calculate all the amplifier properties of in-

 

terest, including spectral and temporal correlations.

We begin in Sec. II by describing the basic model. The main characteristics of the amplifier are embodied in relationships between the input and output photon destruction operators which we derive for arbitrary input fields. In Sec. III we present results for the second-order expectation values of the external fields. These enable us to derive spectral relations describing the output field in terms of the input field, where the role of the amplifier is apparent both in the signal gain and in the added noise. We show that the amount of quantum noise necessarily added by the amplifier satisfies the fundamental noise theorem[1] and find the conditions under which this noise is a minimum. In the latter half of Sec. III we apply our results to several types of input light, including coherent, chaotic, and quantum fields. In Sec. IV we derive results for the fourth-order expectation values of the external fields and evaluate the output intensity correlation for the previously mentioned inputs. We construct the second-order coherence of the output fields. In Sec. V we present the integrated detection statistics of the system, performing a homodyne detection experiment and evaluating the signal-to-noise ratios of the outputs deriving from coherent, chaotic, and squeezed inputs. We also consider direct detection of the outputs from coherent, chaotic, and antibunched input fields. In Sec. VI we show how characteristic functionals can be derived and used to obtain complete statistical information for the amplifier output, thus generalizing the second- and fourth-order results given in earlier sections. Finally, in Sec. VII, we conclude with a discussion of our results.

## II. THE MODEL

### A. Solution of the equations of motion

We consider a system composed of an atomic amplifier placed within a high-$Q$ cavity. The cavity supports a single mode of oscillation characterized by its annihilation operator $\hat{a}(t)$ and coupled via mirrors to multimode external fields. The cavity mode obeys the usual commutation relation

$$[\hat{a},\hat{a}^{\dagger}]=1 , \tag{2.1}$$

while for the external modes we take continuous mode fields with commutation relations

$$\begin{aligned}[\hat{a}_{\rm in}(\omega),\hat{a}^{\dagger}_{\rm in}(\omega')]&=[\hat{a}_{\rm out}(\omega),\hat{a}^{\dagger}_{\rm out}(\omega')]\\&=\delta(\omega-\omega') ,\\ [\hat{b}_{\rm in}(\omega),\hat{b}^{\dagger}_{\rm in}(\omega')]&=[\hat{b}_{\rm out}(\omega),\hat{b}^{\dagger}_{\rm out}(\omega')]\\&=\delta(\omega-\omega') ,\end{aligned} \tag{2.2}$$

where $\hat{a}_{\rm in}(\omega)$ and $\hat{a}_{\rm out}(\omega)$ refer to fields incident on, and emergent from, the cavity on the right, and $\hat{b}_{\rm in}(\omega)$ and $\hat{b}_{\rm out}(\omega)$ refer similarly to fields on the left (Fig. 1). The cavity damping rates $\gamma_1$ and $\gamma_2$ are equal to the mirror intensity transmission coefficients multiplied by $c/(2L)$, where $L$ is the cavity length.

The quantum Langevin[12] equation for the system is

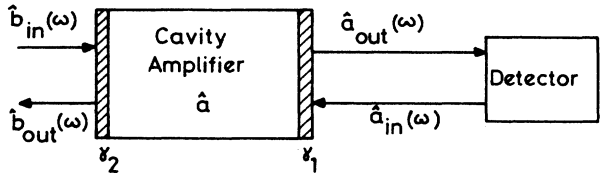


FIG. 1. Schematic arrangement of amplifier and detector showing notation for input and output field operators.

$$\frac{d\hat{a}}{dt}=\frac{-i}{\hbar}[\hat{a},\hat{H}_{\rm sys}]-\tfrac{1}{2}(\gamma_1+\gamma_2)\hat{a}+\hat{\lambda}(t) , \tag{2.3}$$

where $\hat{H}_{\rm sys}$ represents the Hamiltonian for the isolated system in the cavity, and $\hat{\lambda}(t)$ characterizes the noise. This may be ascribed to the fields external to the cavity coupling to the cavity mode through the mirrors[10,11] and we therefore write

$$\hat{\lambda}(t)=\gamma_1^{1/2}\hat{a}_{\rm in}(t)+\gamma_2^{1/2}\hat{b}_{\rm in}(t) . \tag{2.4}$$

If the amplifier is composed of $n_a$ two-level atoms, and if $\hat{\sigma}_j^{-}(t)$ is the lowering operator for the $j$th atom of the amplifier, then the system Hamiltonian $\hat{H}_{\rm sys}$ has the usual form in the rotating-wave and electric-dipole approximations,

$$\hat{H}_{\rm sys}=\hbar\omega_0\hat{a}^{\dagger}\hat{a}+\tfrac{1}{2}\sum_{j=1}^{n_a}\hbar\omega_j\hat{\sigma}_j^{z}+\sum_{j=1}^{n_a}\hbar k_j(\hat{\sigma}_j^{+}\hat{a}+\hat{\sigma}_j^{-}\hat{a}^{\dagger}) , \tag{2.5}$$

where $\hat{\sigma}_j^{z}$ is the atomic inversion operator, $k_j$ is the atom-field coupling constant, $\omega_j$ is the transition frequency of the $j$th atom, and $\omega_0$ is the cavity mode frequency. Substituting this into Eq. (2.3) we obtain the equation for the evolution of the cavity mode,

$$\begin{aligned}\frac{d\hat{a}}{dt}=&-i\omega_0\hat{a}-i\sum_j k_j\hat{\sigma}_j^{-}-\tfrac{1}{2}(\gamma_1+\gamma_2)\hat{a}+\gamma_1^{1/2}\hat{a}_{\rm in}\\&+\gamma_2^{1/2}\hat{b}_{\rm in} .\end{aligned} \tag{2.6}$$

To solve this equation we must first eliminate the atomic operators using the relevant Heisenberg equation,

$$\frac{d\hat{\sigma}_j^{-}}{dt}=-i\omega_j\hat{\sigma}_j^{-}+ik_j\hat{\sigma}_j^{z}\hat{a} . \tag{2.7}$$

We assume that the atomic level populations are externally maintained so that we may make a linearizing approximation, and replace the inversion operator by its expectation value,

$$\hat{\sigma}_j^{z}\rightarrow\langle\hat{\sigma}_j^{z}\rangle=(n_e-n_g)/n_a , \tag{2.8}$$

where $n_e$ and $n_g$ are the numbers of atoms in the excited and ground states, respectively.

The steady-state atomic coherences vanish,

$$\langle\hat{\sigma}_j^{-}\rangle=\langle\hat{\sigma}_j^{+}\rangle=0 . \tag{2.9}$$

The resulting linear equation may be formally solved to give

$$\hat{\sigma}_j^-(t)=\hat{\sigma}_j^-(t_0)e^{-i\omega_j(t-t_0)} +ik_j\langle\hat{\sigma}_j^z\rangle\int_{t_0}^{t}d\tau\, e^{-i\omega_j(t-\tau)}\hat{a}(\tau)\ , \tag{2.10}$$

where $t_0$ is a time in the remote past at which the system is already in a steady state. Defining the Fourier transform of $\hat{a}(t)$ by

$$\hat{a}(\omega)=(2\pi)^{-1/2}\int_{-\infty}^{\infty}dt\, e^{i\omega t}\hat{a}(t) \tag{2.11}$$

and using Eq. (2.10) we find from Eq. (2.6) the result for $\hat{a}(\omega)$,

$$\hat{a}(\omega)=\frac{(2\pi)^{1/2}\sum_j k_j\hat{\sigma}_j^-(t_0)e^{i\omega_j t_0}\delta(\omega-\omega_j)+i\gamma_1^{1/2}\hat{a}_{\rm in}(\omega)+i\gamma_2^{1/2}\hat{b}_{\rm in}(\omega)}{\omega-\omega_0+i\Gamma}\ , \tag{2.12}$$

where

$$\Gamma=\tfrac{1}{2}(\gamma_1+\gamma_2)-(n_e-n_g)\gamma_A\ , \qquad \gamma_A=\frac{\pi k^2(\omega_0)\rho(\omega_0)}{n_a}\ . \tag{2.13}$$

Here, $k(\omega_j)$ is the coupling strength regarded as a function of atomic frequency $\omega_j$, and $\rho(\omega_j)$ the number density of atoms with transition frequency equal to $\omega_j$. Note that we have assumed that both $k$ and $\rho$ are *weakly* dependent on $\omega$ so that the statistical distribution of the atomic population is largely unchanged by its interaction with the cavity mode.[2] In deriving Eq. (2.12), we have made use of the Wigner-Weisskopf approximation.[2]

We may now use the boundary conditions at the cavity mirrors, which take the form

$$\hat{a}(\omega)=\gamma_1^{-1/2}[\hat{a}_{\rm in}(\omega)+\hat{a}_{\rm out}(\omega)] =\gamma_2^{-1/2}[\hat{b}_{\rm in}(\omega)+\hat{b}_{\rm out}(\omega)]\ , \tag{2.14}$$

to recast the result (2.12) expressly in terms of the inputs and outputs to the cavity. Thus, after eliminating the internal mode, we find

$$\hat{a}_{\rm out}(\omega)=-\hat{a}_{\rm in}(\omega)+\frac{(2\pi\gamma_1)^{1/2}\sum_j k_j\hat{\sigma}_j^-(t_0)e^{i\omega_j t_0}\delta(\omega-\omega_j)+i\gamma_1\hat{a}_{\rm in}(\omega)+i(\gamma_2\gamma_2)^{1/2}\hat{b}_{\rm in}(\omega)}{\omega-\omega_0+i\Gamma}\ . \tag{2.15}$$

This is consistent with the commutators (2.2) and the usual atomic commutators

$$[\hat{\sigma}_i^+,\hat{\sigma}_j^-]=\hat{\sigma}_j^z\delta_{ij},\quad [\hat{\sigma}_i^\pm,\hat{\sigma}_j^z]=\mp2\hat{\sigma}_j^\pm\delta_{ij}\ , \tag{2.16}$$

within the range of validity of the linearizing approximation (2.8). Equation (2.15) describes the output field as consisting of both reflected and amplified input contributions and an atomic part which we will identify with the amplifier spontaneous emission. Clearly, in the absence of any input, only this latter term contributes to any measurements made on the output. The effects of the amplifier and cavity are contained in the various detunings and damping rates. This is an entirely general result since we have yet to choose the nature of our input fields.

### B. Time-dependent operator relations

The input-output relation (2.15) may be used to provide all the required amplifier and output field properties. However, it is sometimes useful to work with the transformed version where the operators are explicitly time dependent and defined by, for example,

$$\hat{a}_{\rm out}(t)=(2\pi)^{-1/2}\int_{-\infty}^{\infty}d\omega\, e^{-i\omega t}\hat{a}_{\rm out}(\omega)\ . \tag{2.17}$$

Strictly the range of $\omega$ here extends only from zero to infinity, but an extension of the lower limit down to $-\infty$ is approximately valid if the input states have bandwidth much smaller than $\omega_0$. Then the Fourier transform of Eq. (2.15) is

$$\hat{a}_{\rm out}(t)=-\hat{a}_{\rm in}(t)+\gamma_1^{1/2}\sum_j\frac{k_j\hat{\sigma}_j^-(t_0)e^{-i\omega_j(t-t_0)}}{\omega_j-\omega_0+i\Gamma}+\int_{-\infty}^{t}d\tau\, e^{-(i\omega_0+\Gamma)(t-\tau)}[\gamma_1\hat{a}_{\rm in}(\tau)+(\gamma_1\gamma_2)^{1/2}\hat{b}_{\rm in}(\tau)]\ . \tag{2.18}$$

The time-dependent operators all satisfy commutators of the form

$$[\hat{a}_{\rm out}(t),\hat{a}_{\rm out}^\dagger(t')]=\delta(t-t')\ , \tag{2.19}$$

where the linearizing approximation (2.8) is again employed. Equation (2.18) or its Fourier-transformed equivalent, Eq. (2.15), contains all the information that it is necessary to know in order to investigate the properties of the system.

## III. SECOND-ORDER EXPECTATION VALUES

### A. Spectral functions

It is straightforward to show from Eq. (2.15) that the first-order correlation function of the output field for an arbitrary input is given by

$$\langle \hat{a}^{\dagger}_{\text{out}}(\omega)\hat{a}_{\text{out}}(\omega')\rangle = \frac{2n_e\gamma_1\gamma_A\delta(\omega-\omega')}{(\omega-\omega_0)^2+\Gamma^2} + \frac{\gamma_1\gamma_2\langle \hat{b}^{\dagger}_{\text{in}}(\omega)\hat{b}_{\text{in}}(\omega')\rangle}{(\omega-\omega_0-i\Gamma)(\omega'-\omega_0+i\Gamma)} , \tag{3.1}$$

where the input modes described by $\hat{a}_{\text{in}}(\omega)$ are taken to be unexcited. Consider an input which is stationary in time, with an input frequency correlation given by

$$\langle \hat{b}^{\dagger}_{\text{in}}(\omega)\hat{b}_{\text{in}}(\omega')\rangle = 2\pi f_{\text{in}}(\omega)\delta(\omega-\omega') , \tag{3.2}$$

where $f_{\text{in}}(\omega)$ is the input spectral flux. [The spectral functions $f(\omega)$ represent beam fluxes in terms of photons per unit time per unit angular frequency bandwidth, and are therefore dimensionless quantities.] We find from Eq. (3.1) an output correlation of the form

$$\langle \hat{a}^{\dagger}_{\text{out}}(\omega)\hat{a}_{\text{out}}(\omega')\rangle = 2\pi f_{\text{out}}(\omega)\delta(\omega-\omega') , \tag{3.3}$$

where

$$f_{\text{out}}(\omega) = G(\omega)f_{\text{in}}(\omega) + f_{\text{ch}}(\omega) . \tag{3.4}$$

Here $G(\omega)$ is the amplifier gain at frequency $\omega$, being a maximum for a resonant input,

$$G(\omega) = \frac{\gamma_1\gamma_2}{(\omega-\omega_0)^2+\Gamma^2} , \tag{3.5}$$

while

$$f_{\text{ch}}(\omega) = \frac{n_e\gamma_1\gamma_A/\pi}{(\omega-\omega_0)^2+\Gamma^2} . \tag{3.6}$$

Clearly, in the absence of any input, the output flux is just the chaotic contribution due to spontaneous emission within the amplifier. The total chaotic flux is defined as

$$f_{\text{ch}} = \int_{-\infty}^{\infty} f_{\text{ch}}(\omega)d\omega = \frac{n_e\gamma_1\gamma_A}{\Gamma} . \tag{3.7}$$

Maximum gain occurs at resonance, $\omega=\omega_0$,

$$G(\omega_0) \equiv G_0 = \frac{\gamma_1\gamma_2}{\Gamma^2} . \tag{3.8}$$

The amplifier is assumed to be operated with a peak gain greater than unity ($G_0 > 1$) but below the threshold for self-sustaining laser action ($\Gamma > 0$) so that the population inversion ($n_e - n_g$) must satisfy

$$\tfrac{1}{2}[\gamma_1^{1/2}-\gamma_2^{1/2}]^2 < (n_e-n_g)\gamma_A < \tfrac{1}{2}(\gamma_1+\gamma_2) . \tag{3.9}$$

For an empty cavity ($\gamma_A=0$, $f_{\text{ch}}=0$), Eq. (3.4) becomes

$$f_{\text{out}}(\omega) = \frac{\gamma_1\gamma_2}{(\omega-\omega_0)^2+\frac{1}{4}(\gamma_1+\gamma_2)^2} f_{\text{in}}(\omega) , \tag{3.10}$$

which is the usual Fabry-Pérot input-output spectral relation in the single-mode approximation.[13,14] Note that Eq. (3.9) cannot be satisfied for an empty cavity.

### B. Noise minimization

We will shortly apply the result (3.1) to evaluate the correlation after processing of a number of different input states. First, however, we consider the conditions under which the system may best be operated to minimize the noise flux necessarily generated by the amplifier.

Suppose again that $\hat{b}_{\text{in}}(\omega)$ represents the signal-carrying mode and that $\hat{a}_{\text{out}}(\omega)$ is the output mode of interest. Then Eq. (2.15) can be written

$$\hat{a}_{\text{out}}(\omega) = M(\omega)\hat{b}_{\text{in}}(\omega) + \hat{F}(\omega) , \tag{3.11}$$

where

$$M(\omega) = i(\gamma_1\gamma_2)^{1/2}/(\omega-\omega_0+i\Gamma) \tag{3.12}$$

and the noise operator is

$$\hat{F}(\omega) = \frac{(2\pi\gamma_1)^{1/2}\sum_j k_j\hat{\sigma}_j^- e^{i\omega_j t_0}\delta(\omega-\omega_j) - (\omega-\omega_0+i\Gamma-i\gamma_1)\hat{a}_{\text{in}}(\omega)}{(\omega-\omega_0+i\Gamma)} . \tag{3.13}$$

Making the linearizing approximation (2.8) again, it is easily shown that

$$[\hat{F}(\omega),\hat{F}^{\dagger}(\omega')] = [1-G(\omega)]\delta(\omega-\omega') , \tag{3.14}$$

where $G(\omega)=|M(\omega)|^2$ in agreement with Eq. (3.5). Then using the properties of the noise operator and the results (2.13) and (3.6), it follows that

$$\langle \hat{F}^{\dagger}(\omega')\hat{F}(\omega)\rangle = 2\pi f_{\text{ch}}(\omega)\delta(\omega-\omega') \geq [G(\omega)-1]\delta(\omega-\omega') , \tag{3.15}$$

when the input field $\hat{a}_{\text{in}}(\omega)$ is assumed to be unexcited. This inequality is equivalent to Caves's fundamental theorem[1] for multimode linear amplifiers, and it confirms that our system operates within the standard limits imposed by quantum mechanics.

If we now substitute the explicit forms for the chaotic flux, Eq. (3.6), and the gain, Eq. (3.5), into the inequality (3.15), we find

$$\frac{2n_e\gamma_1\gamma_A}{(\omega-\omega_0)^2+\Gamma^2} \geq \frac{\gamma_1\gamma_2}{(\omega-\omega_0)^2+\Gamma^2} - 1 . \tag{3.16}$$

For resonant inputs $\omega=\omega_0$ (the most stringent regime of the inequality), the theorem reduces to

$$P \geq 1 , \tag{3.17}$$

where

$$P=\frac{2n_e\gamma_1\gamma_A}{\gamma_1\gamma_2-\Gamma^2} , \tag{3.18}$$

since, from Eq. (3.8), $\gamma_1\gamma_2 > \Gamma^2$ for amplification.

Using the expression (2.13) for $\Gamma$, $P$ has a minimum value for the choice of $\gamma_2$ given by

$$\tfrac{1}{2}(\gamma_2-\gamma_1)=(n_e-n_g)\gamma_A . \tag{3.19}$$

Thus minimum added noise is obtained with the input mirror (the mirror through which the input enters the cavity) more highly transmitting than the output mirror. If we were to consider the alternative situation, where $\hat{a}_{\text{in}}$ describes the input and $\hat{b}_{\text{out}}$ the relevant output, then we would again obtain Eq. (3.19) but with the positions of $\gamma_1$ and $\gamma_2$ reversed. The result (3.19) is therefore asymmetric in the mirror transmissivities but symmetric with respect to the whole system. This would appear contrary to intuition derived from familiarity with Fabry-Pérot cavities, where perfect transmission of a resonant input is obtained with identical mirrors, and is independent of the chosen direction of throughput. However, a Fabry-Pérot cavity is a passive, time-reversible system. Our system includes an amplifier which is most definitely not time-reversible: were it to be run backwards the amplifier would not reabsorb the existing spontaneously emitted photons, but would only produce more.[15] It is clearly the amplifier asymmetry which results in the need for mirror asymmetry: setting $\gamma_A$ (essentially the field-atom coupling) equal to zero in Eq. (3.19), and thereby removing the amplifier, leads to $\gamma_1=\gamma_2$, as one would expect. The degree of asymmetry needed is directly proportional to the degree of population inversion in the amplifier, $(n_e-n_g)$. This is not surprising since the greater the inversion the greater the spontaneous emission, and from Eq. (3.6) it is precisely the spontaneous emission which is responsible for the noise on the output (recalling that $\hat{a}_{\text{in}}$ describes a vacuum field). Reducing the output mirror transmissivity with respect to that of the input mirror according to Eq. (3.19) thus essentially reduces the number of noise photons in the detected output beam.

Choosing, then, an asymmetric cavity, the result for $P$ is

$$P=\frac{n_e}{n_e-n_g} , \tag{3.20}$$

which is seen to be simply the population factor that appears in the theory of the discrete mode amplifier.[5] The cavity amplifier decay rate given in Eq. (2.13) reduces to

$$\Gamma=\gamma_1 \tag{3.21}$$

and the gain, from Eq. (3.8), becomes

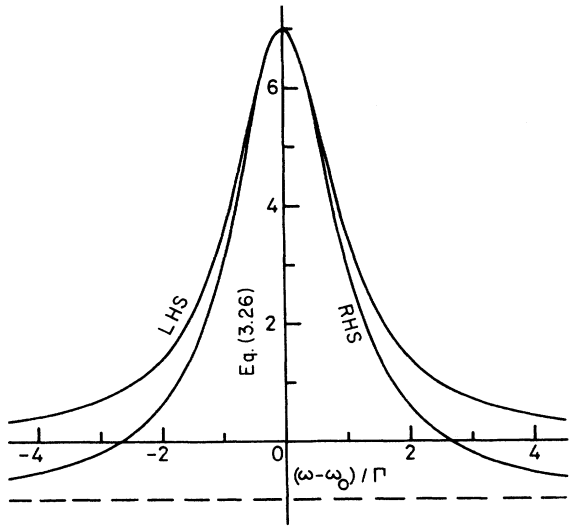


FIG. 2. Illustration of the inequality (3.26) for a peak gain $G_0=8$. The upper Lorentzian curve represents the frequency-dependent noise from the left-hand side of Eq. (3.26), while the lower curve represents the frequency-dependent gain minus 1 from the right-hand side of Eq. (3.26).

$$G(\omega_0)=\frac{\gamma_2}{\gamma_1}=1+\frac{2(n_e-n_g)\gamma_A}{\gamma_1} , \tag{3.22}$$

which increases with increasing inversion and coupling strength and with decreasing output transmittance. It is clear from the form of $P$ in Eq. (3.20) that the inequality (3.17) is indeed satisfied. Minimum noise ($P=1$) occurs for $n_e=n_a$, $n_g=0$, when the mirror decay rates are highly asymmetric,

$$\gamma_2=\gamma_1+2n_a\gamma_A \tag{3.23}$$

and the gain is

$$G(\omega_0)=1+\frac{2n_a\gamma_A}{\gamma_1} . \tag{3.24}$$

In this regime, the total chaotic flux (3.7) is related to the peak chaotic flux and peak gain by

$$\frac{f_{\text{ch}}}{\Gamma}=\pi f_{\text{ch}}(\omega_0)=\tfrac{1}{2}(G_0-1) \tag{3.25}$$

and Eq. (3.16) can be written

$$\frac{G_0-1}{[(\omega-\omega_0)/\Gamma]^2+1} \geq \frac{G_0}{[(\omega-\omega_0)/\Gamma]^2+1}-1 . \tag{3.26}$$

The inequality (3.26) is illustrated in Fig. 2.

### C. Temporal correlation functions

The Fourier transform of the output spectral function (3.1) is defined by

$$\langle \hat{a}^{\dagger}_{\rm out}(t)\hat{a}_{\rm out}(t')\rangle = (2\pi)^{-1}\int_{-\infty}^{\infty} d\omega \int_{-\infty}^{\infty} d\omega' e^{i\omega t - i\omega' t'}\langle \hat{a}^{\dagger}_{\rm out}(\omega)\hat{a}_{\rm out}(\omega')\rangle \tag{3.27}$$

and we define the time-dependent output flux to be

$$f_{\rm out}(t) = \langle \hat{a}^{\dagger}_{\rm out}(t)\hat{a}_{\rm out}(t)\rangle \ . \tag{3.28}$$

If we consider input fields with time-stationary statistical properties, so that Eq. (3.3) holds, then the expression for the output temporal correlation (3.27) reduces to

$$\langle \hat{a}^{\dagger}_{\rm out}(t)\hat{a}_{\rm out}(t')\rangle = \int_{-\infty}^{\infty} d\omega\, e^{i\omega(t-t')} f_{\rm out}(\omega) \ . \tag{3.29}$$

For the output flux we find

$$f_{\rm out}(t) = \int_{-\infty}^{\infty} d\omega\, f_{\rm out}(\omega) \equiv f_{\rm out} \ , \tag{3.30}$$

which is time independent.

In general, with the output field described by Eq. (2.18), the output second-order correlation function is

$$\langle \hat{a}^{\dagger}_{\rm out}(t)\hat{a}_{\rm out}(t')\rangle = f_{\rm ch} e^{i\omega_0(t-t')-\Gamma|t-t'|} + \gamma_1\gamma_2 \int_{-\infty}^{t} d\tau \int_{-\infty}^{t'} d\tau' e^{(i\omega_0-\Gamma)(t-\tau)-(i\omega_0+\Gamma)(t'-\tau')}\langle \hat{b}^{\dagger}_{\rm in}(\tau)\hat{b}_{\rm in}(\tau')\rangle \ , \tag{3.31}$$

where the chaotic output flux is given by Eq. (3.7) and the modes represented by $\hat{a}_{\rm in}$ are assumed to be unexcited. The total output flux is thus

$$f_{\rm out}(t) = f_{\rm ch} + \gamma_1\gamma_2 \int\int_{-\infty}^{t} d\tau\, d\tau' e^{-i\omega_0(\tau-\tau')-\Gamma(2t-\tau-\tau')}\langle \hat{b}^{\dagger}_{\rm in}(\tau)\hat{b}_{\rm in}(\tau')\rangle \ , \tag{3.32}$$

which is simply the sum of the input flux after amplification and the spontaneous-emission flux. For a stationary input, whose correlation depends only on the time difference $\tau-\tau'$, we may conveniently change the variables to

$$\begin{aligned} \sigma &= \tau - \tau' \ , \\ s &= \tau + \tau' - 2t \ , \end{aligned} \tag{3.33}$$

and perform the integration over $s$ to find

$$f_{\rm out} = f_{\rm ch} + \frac{\gamma_1\gamma_2}{2\Gamma}\int_{-\infty}^{\infty} d\sigma\, e^{-i\omega_0\sigma-\Gamma|\sigma|}\langle \hat{b}^{\dagger}_{\rm in}(\sigma)\hat{b}_{\rm in}(0)\rangle \ . \tag{3.34}$$

We now apply these results in evaluating the output correlation associated with particular inputs.

### D. Results for specific inputs

#### 1. Coherent input

A coherent input state can be defined by

$$|\{\beta_{\rm in}(\omega)\}\rangle = \exp\left[\int_{-\infty}^{\infty} d\omega [\beta_{\rm in}(\omega)\hat{b}^{\dagger}_{\rm in}(\omega) - \beta^{*}_{\rm in}(\omega)\hat{b}_{\rm in}(\omega)]\right]|0\rangle \tag{3.35}$$

and it has the properties

$$\begin{aligned} \hat{b}_{\rm in}(\omega)|\{\beta_{\rm in}(\omega)\}\rangle &= \beta_{\rm in}(\omega)|\{\beta_{\rm in}(\omega)\}\rangle \ , \\ \hat{b}_{\rm in}(t)|\{\beta_{\rm in}(\omega)\} &= \beta_{\rm in}(t)|\{\beta_{\rm in}(\omega)\}\rangle \ , \end{aligned} \tag{3.36}$$

where $\beta_{\rm in}(\omega)$ is an arbitrary complex function of $\omega$ and

$$\beta_{\rm in}(t) = (2\pi)^{-1/2}\int_{-\infty}^{\infty} d\omega\, e^{-i\omega t}\beta_{\rm in}(\omega) \ . \tag{3.37}$$

We consider here only a quasi-single-mode coherent-state input, where $\beta_{\rm in}(\omega)$ is a very sharply peaked function,

$$\beta_{\rm in}(\omega) = (2\pi f_{\rm in})^{1/2} e^{i\varphi}\delta(\omega-\omega_c) \tag{3.38}$$

and

$$\beta_{\rm in}(t) = f_{\rm in}^{1/2} e^{-i\omega_c t + i\varphi} \ . \tag{3.39}$$

The spectral correlation function thus describes a time-stationary input as defined by Eq. (3.2), with

$$f_{\rm in}(\omega) = f_{\rm in}\delta(\omega-\omega_c) \tag{3.40}$$

and the total input flux is simply

$$\langle \hat{b}^{\dagger}_{\rm in}(t)\hat{b}_{\rm in}(t)\rangle = f_{\rm in} \ . \tag{3.41}$$

The output spectral function (3.4) in this case is

$$f_{\rm out}(\omega) = G(\omega) f_{\rm in}\delta(\omega-\omega_c) + f_{\rm ch}(\omega) \tag{3.42}$$

and it shows an amplified coherent $\delta$-function peak superimposed on a continuous chaotic background. Also, using

$$\langle \hat{b}^{\dagger}_{\rm in}(t)\hat{b}_{\rm in}(t')\rangle = f_{\rm in} e^{i\omega_c(t-t')} \tag{3.43}$$

the total output flux can be obtained from (3.34) as

$$f_{\rm out} = f_{\rm ch} + \frac{\gamma_1\gamma_2 f_{\rm in}}{(\omega_c-\omega_0)^2+\Gamma^2} = f_{\rm ch} + G(\omega_c) f_{\rm in} \ , \tag{3.44}$$

with $G(\omega)$ as defined in Eq. (3.5). This is precisely the form one would expect from a true (quantum-mechanical) amplifier.[16] More generally, the output correlation (3.31) is, using Eq. (3.43),

$$\langle \hat{a}^{\dagger}_{\rm out}(t)\hat{a}_{\rm out}(t')\rangle = f_{\rm ch} e^{i\omega_0(t-t')-\Gamma|t-t'|} + G(\omega_c) f_{\rm in} e^{i\omega_c(t-t')} \ . \tag{3.45}$$

This is the typical result for a superposition of chaotic and coherent light.[17] The above results also hold gen-

erally for any input whose frequency spread is much smaller than $\Gamma$, the system bandwidth.

### 2. Chaotic input

Consider chaotic input light with a Lorentzian frequency spread of linewidth $\gamma_c$, centered on a frequency $\omega_c$. The spectral correlation function is given by Eq. (3.2) with

$$f_{\rm in}(\omega)=\frac{(\gamma_c/\pi)f_{\rm in}}{(\omega-\omega_c)^2+\gamma_c^2}\ , \tag{3.46}$$

where $f_{\rm in}$ is the total input flux. The output flux (3.4) has the usual chaotic contribution from the amplifier spontaneous emission together with a product of Lorentzian distributions representing the amplified chaotic input. The time-dependent correlation

$$\langle \hat{b}^{\dagger}_{\rm in}(t)\hat{b}_{\rm in}(t')\rangle=\int_{-\infty}^{\infty}d\omega\, e^{i\omega(t-t')}f_{\rm in}(\omega)\ , \tag{3.47}$$

corresponding to the input flux (3.46) is

$$\langle \hat{b}^{\dagger}_{\rm in}(t)\hat{b}_{\rm in}(t')\rangle=f_{\rm in}e^{i\omega_c(t-t')-\gamma_c|t-t'|}\ . \tag{3.48}$$

The corresponding output correlation is obtained from Eq. (3.31). We consider for simplicity only the special case where the input Lorentzian is centered on the cavity frequency, $\omega_c=\omega_0$, when

$$\langle \hat{a}^{\dagger}_{\rm out}(t)\hat{a}_{\rm out}(t')\rangle=f_{\rm ch}e^{i\omega_0(t-t')-\Gamma|t-t'|}+\frac{\gamma_1\gamma_2 f_{\rm in}}{\Gamma(\Gamma^2-\gamma_c^2)}e^{i\omega_0(t-t')}(\Gamma e^{-\gamma_c|t-t'|}-\gamma_c e^{-\Gamma|t-t'|})\ . \tag{3.49}$$

The total output flux obtained by setting $t=t'$ is

$$f_{\rm out}=f_{\rm ch}+\frac{\gamma_1\gamma_2 f_{\rm in}}{\Gamma(\Gamma+\gamma_c)}=f_{\rm ch}+\left[\frac{\Gamma}{\Gamma+\gamma_c}\right]G_0 f_{\rm in}\ . \tag{3.50}$$

Thus for $\Gamma\gg\gamma_c$,

$$f_{\rm out}=f_{\rm ch}+G_0 f_{\rm in} \tag{3.51}$$

and for $\Gamma\ll\gamma_c$,

$$f_{\rm out}=f_{\rm ch}+\frac{\Gamma}{\gamma_c}G_0 f_{\rm in}\ . \tag{3.52}$$

These features reflect the well-known properties, even of empty Fabry-Pérot cavities [$\gamma_A=0$ in Eq. (2.13)], that the total flux of the output is governed by the smaller of the widths $\gamma_c$ of the input light and $\Gamma$ of the cavity itself.

### 3. Number-state input

Consider an input state defined by[18]

$$|\{n,t_0\}\rangle=\prod_{n=-\infty}^{\infty}\hat{A}^{\dagger}(\beta_n)|0\rangle\ , \tag{3.53}$$

where $n$ takes all integer values and

$$\begin{aligned}\hat{A}^{\dagger}(\beta_n)&=\int_{-\infty}^{\infty}d\omega\,\beta_n(\omega)\hat{b}^{\dagger}_{\rm in}(\omega)\\&=\int_{-\infty}^{\infty}dt\,\beta_n(t)\hat{b}^{\dagger}_{\rm in}(t)\ .\end{aligned} \tag{3.54}$$

The functions $\beta_n$ are normalized according to

$$\int_{-\infty}^{\infty}d\omega|\beta_n(\omega)|^2=\int_{-\infty}^{\infty}dt|\beta_n(t)|^2=1 \tag{3.55}$$

and with the choice

$$\beta_n(\omega)=\frac{(\gamma/\pi)^{1/2}}{\omega-\omega_0+i\gamma}e^{i\omega nt_0} \tag{3.56}$$

or, equivalently,

$$\beta_n(t)=-i(2\gamma)^{1/2}e^{-(i\omega_0+\gamma)(t-nt_0)}\Theta(t-nt_0)\ , \tag{3.57}$$

the state (3.53) represents an infinite chain of single-photon pulses with equal spacing $t_0$. Note that the state $|\{n,t_0\}\rangle$, as defined in Eq. (3.53), is unnormalized. The condition $\gamma t_0\gg 1$, however, which ensures that the pulses are well separated and have negligible time overlap, can be shown to reduce the normalization constant to unity when the infinite product of Eq. (3.53) is defined as the limit of a *finite* product. These conditions will be assumed in the following. The integrated creation and destruction operators defined by Eq. (3.54) and its Hermitian conjugate satisfy the commutation relations

$$\begin{aligned}&[\hat{b}_{\rm in}(\omega),\hat{A}^{\dagger}(\beta_n)]=\beta_n(\omega)\ ,\\&[\hat{b}_{\rm in}(t),\hat{A}^{\dagger}(\beta_n)]=\beta_n(t)\ ,\end{aligned} \tag{3.58}$$

and

$$[\hat{A}(\beta_n),\hat{A}^{\dagger}(\beta_{n'})]=\delta_{n,n'}\ . \tag{3.59}$$

The second-order expectation values for the state (3.53), obtained with the use of the commutators, are

$$\langle \hat{b}^{\dagger}_{\rm in}(\omega)\hat{b}_{\rm in}(\omega')\rangle=\sum_{n=-\infty}^{\infty}\beta_n^*(\omega)\beta_n(\omega') \tag{3.60}$$

and

$$\langle \hat{b}^{\dagger}_{\rm in}(t)\hat{b}_{\rm in}(t')\rangle=\sum_{n=-\infty}^{\infty}\beta_n^*(t)\beta_n(t')\ . \tag{3.61}$$

Thus the time-dependent input flux is

$$\begin{aligned}f_{\rm in}(t)&=\langle \hat{b}^{\dagger}_{\rm in}(t)\hat{b}_{\rm in}(t)\rangle\\&=\sum_{n=-\infty}^{\infty}2\gamma e^{-2\gamma(t-nt_0)}\Theta(t-nt_0)\ .\end{aligned} \tag{3.62}$$

This is clearly not time stationary. The mean input flux is given by a long-time average (denoted here by the subscript "av") of Eq. (3.62) as

$$(f_{\rm in})_{\rm av}=\lim_{T_0\to\infty}\frac{1}{T_0}\int_0^{T_0}f_{\rm in}(t)dt=\frac{1}{t_0}\ . \tag{3.63}$$

The output spectral correlation function can be found from Eq. (3.31) using Eq. (3.61) as

$$\langle \hat{a}^{\dagger}_{\rm out}(t)\hat{a}_{\rm out}(t')\rangle = e^{i\omega_0(t-t')}\left[f_{\rm ch}e^{-\Gamma|t-t'|}+\frac{2\gamma\gamma_1\gamma_2}{(\Gamma-\gamma)^2}\sum_{n=-\infty}^{\infty}(e^{-\Gamma(t-nt_0)}-e^{-\gamma(t-nt_0)})(e^{-\Gamma(t'-nt_0)}-e^{-\gamma(t'-nt_0)})\right.$$
$$\left.\times\Theta(t-nt_0)\Theta(t'-nt_0)\right] . \tag{3.64}$$

It is again seen that the time dependence of the second term of the output correlation (3.64) is mainly governed by the smaller of $\gamma$ and $\Gamma$, when these have very different magnitudes. The total output flux is

$$f_{\rm out}(t)=\langle \hat{a}^{\dagger}_{\rm out}(t)\hat{a}_{\rm out}(t)\rangle$$
$$=f_{\rm ch}+\frac{2\gamma\gamma_1\gamma_2}{(\Gamma-\gamma)^2}\sum_{n=-\infty}^{\infty}(e^{-\Gamma(t-nt_0)}-e^{-\gamma(t-nt_0)})^2\Theta(t-nt_0) . \tag{3.65}$$

A long-time average, analogous to Eq. (3.63), gives the mean output flux

$$(f_{\rm out})_{\rm av}=f_{\rm ch}+\frac{\gamma_1\gamma_2}{\Gamma(\Gamma+\gamma)}(f_{\rm in})_{\rm av} , \tag{3.66}$$

which may be compared to the chaotic result (3.50), and which takes similar limiting values. The reason for the strong likeness between the results for chaotic and for number-state inputs is that both were arbitrarily chosen to have Lorentzian spectral distributions, (3.46) and (3.60). However, sharp differences emerge when the fourth-order correlation functions are studied.

## IV. FOURTH-ORDER EXPECTATION VALUES

### A. Intensity correlation functions

We consider the normally-ordered correlation of the output intensity, which is related to the input correlations via Eq. (2.18) in the form

$$\langle \hat{a}^{\dagger}_{\rm out}(t')\hat{a}^{\dagger}_{\rm out}(t)\hat{a}_{\rm out}(t)\hat{a}_{\rm out}(t')\rangle$$
$$=f_{\rm ch}^2(1+e^{-2\Gamma|t-t'|})$$
$$+\gamma_1\gamma_2 f_{\rm ch}\left[e^{-\Gamma|t-t'|}\int_{-\infty}^{t}d\tau\int_{-\infty}^{t'}d\tau' e^{-\Gamma(t-\tau+t'-\tau')}[e^{i\omega_0(\tau-\tau')}\langle \hat{b}^{\dagger}_{\rm in}(\tau')\hat{b}_{\rm in}(\tau)\rangle+e^{-i\omega_0(\tau-\tau')}\langle \hat{b}^{\dagger}_{\rm in}(\tau)\hat{b}_{\rm in}(\tau')\rangle]\right.$$
$$+\int_{-\infty}^{t}d\tau\int_{-\infty}^{t}d\tau' e^{i\omega_0(\tau-\tau')-\Gamma(2t-\tau-\tau')}\langle \hat{b}^{\dagger}_{\rm in}(\tau')\hat{b}_{\rm in}(\tau)\rangle$$
$$\left.+\int_{-\infty}^{t'}d\tau\int_{-\infty}^{t'}d\tau' e^{-i\omega_0(\tau-\tau')-\Gamma(2t'-\tau-\tau')}\langle \hat{b}^{\dagger}_{\rm in}(\tau)\hat{b}_{\rm in}(\tau')\rangle\right]$$
$$+\gamma_1^2\gamma_2^2\int_{-\infty}^{t}d\tau\int_{-\infty}^{t'}d\tau'\int_{-\infty}^{t'}d\tau''\int_{-\infty}^{t}d\tau''' e^{-i\omega_0(\tau+\tau'-\tau''-\tau''')-\Gamma(2t+2t'-\tau-\tau'-\tau''-\tau''')}$$
$$\times\langle \hat{b}^{\dagger}_{\rm in}(\tau)\hat{b}^{\dagger}_{\rm in}(\tau')\hat{b}_{\rm in}(\tau'')\hat{b}_{\rm in}(\tau''')\rangle . \tag{4.1}$$

We are also interested in the output degree of second-order coherence, which, for stationary light beams, is defined by

$$g^{(2)}_{\rm out}(t)=\frac{\langle \hat{a}^{\dagger}_{\rm out}(0)\hat{a}^{\dagger}_{\rm out}(t)\hat{a}_{\rm out}(t)\hat{a}_{\rm out}(0)\rangle}{\langle \hat{a}^{\dagger}_{\rm out}(0)\hat{a}_{\rm out}(0)\rangle^2} , \tag{4.2}$$

with a similar expression $g^{(2)}_{\rm in}(t)$ for the input field.

### B. Results for specific inputs

#### 1. Coherent input

The input state $|\{\beta_{\rm in}(\omega)\}\rangle$ specified by Eqs. (3.36) and (3.38) has a degree of second-order coherence

$$g^{(2)}_{\rm in}(t)=1 . \tag{4.3}$$

The output beam is also stationary, with the correlation given by Eq. (4.1) as

$$\langle \hat{a}^{\dagger}_{\rm out}(0)\hat{a}^{\dagger}_{\rm out}(t)\hat{a}_{\rm out}(t)\hat{a}_{\rm out}(0)\rangle=f_{\rm ch}^2(1+e^{-2\Gamma|t|})+2f_{\rm ch}G(\omega_c)f_{\rm in}[1+e^{-\Gamma|t|}\cos(\omega_c-\omega_0)t]+G^2(\omega_c)f_{\rm in}^2 . \tag{4.4}$$

We therefore find for the second-order coherence (4.2) in the case $t=0$ and $\omega_c=\omega_0$ the result

$$g^{(2)}_{\rm out}(0)=\frac{2f^2_{\rm ch}+4f_{\rm ch}G_0f_{\rm in}+G_0^2f^2_{\rm in}}{(f_{\rm ch}+G_0f_{\rm in})^2}$$
$$=1+\frac{f^2_{\rm ch}+2f_{\rm ch}G_0f_{\rm in}}{(f_{\rm ch}+G_0f_{\rm in})^2}\ , \tag{4.5}$$

where we have used Eq. (3.44). This is the well-known result[5] for the degree of second-order coherence for a superposition of chaotic light of flux $f_{\rm ch}$ and coherent light of flux $G_0f_{\rm in}$. Clearly $g^{(2)}_{\rm out}(0)$ can never be less than 1, and if the input is removed Eq. (4.5) collapses to the chaotic value of 2, so that, in general, the amplification process degrades the signal.

### 2. Chaotic input

Considering a chaotic input field, with the Lorentzian spectrum (3.46), we find the following correlation function:

$$\langle \hat b^\dagger_{\rm in}(t')\hat b^\dagger_{\rm in}(t)\hat b_{\rm in}(t)\hat b_{\rm in}(t')\rangle=f^2_{\rm in}(1+e^{-2\gamma_c|t-t'|})\ . \tag{4.6}$$

The field is stationary in time and thus the degree of second-order coherence is

$$g^{(2)}_{\rm in}(t)=1+e^{-2\gamma_c|t|}\ , \tag{4.7}$$

which is the usual form for chaotic light.[19] We evaluate the output intensity correlation considering for simplicity only the case where the input Lorentzian is centered on the cavity mode frequency ($\omega_c=\omega_0$), and then Eq. (4.1) gives

$$\langle \hat a^\dagger_{\rm out}(0)\hat a^\dagger_{\rm out}(t)\hat a_{\rm out}(t)\hat a_{\rm out}(0)\rangle=f^2_{\rm ch}(1+e^{-2\Gamma|t|})+2\gamma_1\gamma_2f_{\rm ch}f_{\rm in}\left[e^{-\Gamma|t|}\frac{(\Gamma e^{-\gamma_c|t|}-\gamma_c e^{-\Gamma|t|})}{\Gamma(\Gamma^2-\gamma_c^2)}+\frac{1}{\Gamma(\Gamma+\gamma_c)}\right]$$
$$+\gamma_1^2\gamma_2^2f^2_{\rm in}\left[\frac{(\Gamma e^{-\gamma_c|t|}-\gamma_c e^{-\Gamma|t|})^2}{\Gamma^2(\Gamma^2-\gamma_c^2)^2}+\frac{1}{\Gamma^2(\Gamma+\gamma_c)^2}\right]\ . \tag{4.8}$$

This result can be recast in terms of the first-order correlation (3.49) as

$$\langle \hat a^\dagger_{\rm out}(0)\hat a^\dagger_{\rm out}(t)\hat a_{\rm out}(t)\hat a_{\rm out}(0)\rangle$$
$$=|\langle \hat a^\dagger_{\rm out}(0)\hat a_{\rm out}(0)\rangle|^2+|\langle \hat a^\dagger_{\rm out}(t)\hat a_{\rm out}(0)\rangle|^2 \tag{4.9}$$

and the output is purely chaotic. Equation (4.8) describes the superposition of two chaotic fields, one the input and one the amplifier noise, and Eq. (4.9) is a familiar result.[19] The input and output degrees of second-order coherence thus both take the value 2 at $t=0$,

$$g^{(2)}_{\rm in}(0)=g^{(2)}_{\rm out}(0)=2\ . \tag{4.10}$$

### 3. Number-state input

We consider again the stream of photons defined by Eqs. (3.5)–(3.57). Before processing, the field has a second-order correlation

$$\langle \hat b^\dagger_{\rm in}(t')\hat b^\dagger_{\rm in}(t)\hat b_{\rm in}(t)\hat b_{\rm in}(t')\rangle$$
$$=\sum_{n,n'=-\infty}^{\infty}{}'\ |\beta_n(t)|^2|\beta_{n'}(t')|^2\ , \tag{4.11}$$

where we have made use of the commutation relation (3.58), and the prime on the summation indicates that terms with $n'=n$ are excluded. Using the explicit form in Eq. (3.57) of the functions $\beta_n$ we find

$$\langle \hat b^\dagger_{\rm in}(t')\hat b^\dagger_{\rm in}(t)\hat b_{\rm in}(t)\hat b_{\rm in}(t')\rangle$$
$$=\sum_{n,n'=-\infty}^{\infty}{}'\ 4\gamma^2e^{-2\gamma(t-nt_0+t'-n't_0)}\Theta(t-nt_0)$$
$$\times\Theta(t'-n't_0)\ . \tag{4.12}$$

This describes a highly nonstationary field, and it is convenient again to take a long-time average, analogous to Eq. (3.63). For a fixed time difference $t'-t$, averaging over $t$ gives

$$\langle \hat b^\dagger_{\rm in}(t')\hat b^\dagger_{\rm in}(t)\hat b_{\rm in}(t)\hat b_{\rm in}(t')\rangle_{\rm av}$$
$$=(\gamma/t_0)\sum_{n=1}^{\infty}e^{-2\gamma||t'-t|-nt_0|}\ . \tag{4.13}$$

Using Eq. (3.63), the time-averaged degree of second-order coherence of the input becomes

$$g^{(2)}_{\rm in}(t)=\gamma t_0\sum_{n=1}^{\infty}e^{-2\gamma||t|-nt_0|}\ . \tag{4.14}$$

It follows from the assumption $\gamma t_0\gg1$ that

$$g^{(2)}_{\rm in}(0)=0\ , \tag{4.15}$$

indicating a fully antibunched field. The function (4.14) is shown in Fig. 3, and it is zero unless the correlation lag is close to an integer number of photon spacings.

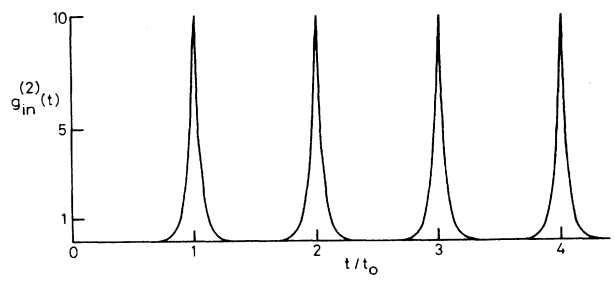


FIG. 3. The time-averaged degree of second-order coherence (4.14) for the photon-number input state, drawn for $\gamma t_0=10$.

Having established that the definitions (3.53)–(3.57) do indeed describe an antibunched field, the interesting question now is whether we can retain these quantum statistical properties after amplification. This is most likely to be achieved when the input pulse spacing $t_0$ is sufficiently large to satisfy the inequality $\Gamma t_0 \gg 1$. This condition corresponds to the situation where only one photon at a time passes through the cavity. The amplified output in this case should consist of separated photon pulses. The opposite limit $\Gamma t_0 \ll 1$ corresponds to many photons simultaneously within the amplifier cavity, so that one might expect the output to consist of photons with a rather random temporal relationship. Since we are interested in the conditions under which we can retain an antibunched output, we assume henceforth that $\Gamma t_0 \gg 1$, together with the previous assumption that $\gamma t_0 \gg 1$.

In addition to the quantum effects of the antibunched input, which tend to reduce the coherence below unity, there is also competition with the added noise photons, which tend to randomize the field and move the coherence towards the chaotic value of 2. There will be some maximum gain beyond which the associated added noise will dominate the output. To investigate this, we first calculate the output correlation from (4.1), finding

$$\begin{aligned}\langle \hat{a}^{\dagger}_{\rm out}(t')\hat{a}^{\dagger}_{\rm out}(t)\hat{a}_{\rm out}(t)\hat{a}_{\rm out}(t')\rangle &= f_{\rm ch}^2(1+e^{-2\Gamma|t-t'|}) \\ &+\frac{2\gamma\gamma_1\gamma_2}{(\Gamma-\gamma)^2}f_{\rm ch}\sum_{n=-\infty}^{\infty}[(e^{-\Gamma(t-nt_0)}-e^{-\gamma(t-nt_0)})(e^{-\Gamma(t'-nt_0)}-e^{-\gamma(t'-nt_0)})2e^{-\Gamma|t-t'|}\Theta(t-nt_0)\Theta(t'-nt_0) \\ &\quad +(e^{-\Gamma(t-nt_0)}-e^{-\gamma(t-nt_0)})^2\Theta(t-nt_0)+(e^{-\Gamma(t'-nt_0)}-e^{-\gamma(t'-nt_0)})^2\Theta(t'-nt_0)] \\ &+\left[\frac{2\gamma\gamma_1\gamma_2}{(\Gamma-\gamma)^2}\right]^2\sum_{n',n=-\infty}^{\infty}{}'(e^{-\Gamma(t-nt_0)}-e^{-\gamma(t-nt_0)})^2(e^{-\Gamma(t'-n't_0)}-e^{-\gamma(t'-n't_0)})^2\Theta(t-nt_0)\Theta(t'-n't_0)\ . \end{aligned} \tag{4.16}$$

As with the input, we assume the time difference $t'-t$ to be fixed, and average over $t$, finding

$$\begin{aligned}\langle \hat{a}^{\dagger}_{\rm out}(t')\hat{a}^{\dagger}_{\rm out}(t)\hat{a}_{\rm out}(t)\hat{a}_{\rm out}(t')\rangle_{\rm av} &= f_{\rm ch}^2(1+e^{-2\Gamma|t'-t|})+\frac{2\gamma_1\gamma_2}{\Gamma(\Gamma+\gamma)}f_{\rm ch}(f_{\rm in})_{\rm av}\left[1+\frac{\gamma\Gamma}{\gamma-\Gamma}\left[\frac{e^{-2\Gamma|t'-t|}}{\Gamma}-\frac{e^{-(\gamma+\Gamma)|t'-t|}}{\gamma}\right]\right] \\ &+\left[\frac{2\gamma\gamma_1\gamma_2}{\Gamma-\gamma}\right]^2\frac{(f_{\rm in})_{\rm av}}{\Gamma+\gamma}\sum_{n=1}^{\infty}\left[\frac{e^{-2\Gamma||t'-t|-nt_0|}}{4\Gamma(3\Gamma+\gamma)}+\frac{e^{-2\gamma||t'-t|-nt_0|}}{4\gamma(3\gamma+\Gamma)}-\frac{2e^{-(\gamma+\Gamma)||t'-t|-nt_0|}}{(3\Gamma+\gamma)(3\gamma+\Gamma)}\right]\ . \end{aligned} \tag{4.17}$$

This is more complicated than the equivalent result for the input, Eq. (4.13). However, we may immediately establish a few points. Firstly, if there is no input signal, then, remembering the definition (4.2) of $g^2_{\rm out}(t)$ and that the mean output flux is given by Eq. (3.66), we find the usual chaotic result for the cavity spontaneous-emission field,

$$g^{(2)}_{\rm out}(t)=1+e^{-2\Gamma|t|},\quad (f_{\rm in})_{\rm av}=0\ . \tag{4.18}$$

More generally, in the presence of the number-state input, the degree of second-order coherence is obtained from Eq. (4.2) with insertion of the complete expression (4.17). It is illuminating to consider just the particular case of $t=0$, when we find

$$g^{(2)}_{\rm out}(0)=\frac{2f_{\rm ch}^2+[4\gamma_1\gamma_2/\Gamma(\Gamma+\gamma)]f_{\rm ch}(f_{\rm in})_{\rm av}}{\{f_{\rm ch}+[\gamma_1\gamma_2/\Gamma(\Gamma+\gamma)](f_{\rm in})_{\rm av}\}^2}\ . \tag{4.19}$$

This can be rewritten to obtain the output coherence for the case of minimum noise on the signal. Using Eqs. (3.21), (3.22), (3.25), and (3.63) gives

$$g^{(2)}_{\rm out}(0)=\frac{2(G_0-1)^2+8G_0(G_0-1)/[(\Gamma+\gamma)t_0]}{\{G_0-1+2G_0/[(\Gamma+\gamma)t_0)\}^2}\ . \tag{4.20}$$

This is identical to a previous result[5] describing a single-mode field, provided that we identify our mean photon number $\bar{n}_0$ as

$$\bar{n}_0=\frac{2}{(\Gamma+\gamma)t_0}\ . \tag{4.21}$$

This mean photon number is very small, since $\gamma t_0$ and $\Gamma t_0$ have both been assumed to be much larger than unity. It is not difficult to show from Eq. (4.20) that

$$g^{(2)}_{\rm out}(0)<1\ \text{ if } G_0<1+(2^{1/2}-1)\bar{n}_0\ . \tag{4.22}$$

Thus only very modest amplifier gains are permitted if the input antibunching is to be preserved at the output.

## V. INTEGRATED DETECTION STATISTICS

Before considering what information about the outputs can be gained from homodyne and direct detection mea-

surements of them, we first review briefly some of the results from detection theory that we will need.

### A. Homodyne detection

We consider balanced homodyne detection in which the amplifier output is detected after superposition with a local oscillator beam at a 50/50 beamsplitter. The measured quantity is the difference between the photocounts registered by two detectors placed in the beamsplitter outputs.[20] The local oscillator is a "single-mode" coherence light source described in accordance with Eq. (3.39) by a time-dependent function

$$\beta_L(t)=f_L^{1/2}e^{-i\omega_L t+i\varphi_L} . \tag{5.1}$$

The local oscillator flux is assumed to be very much larger than that of the amplifier output ($f_L \gg f_{\rm out}$) and detected quantities are evaluated to the dominant nonvanishing order in $f_L$.

The homodyne detection characteristics are compactly expressed in terms of expectation values of a quadrature operator defined to be

$$\hat{X}_{\rm out}(\chi_L,t)=\tfrac{1}{2}[\hat{a}^{\dagger}_{\rm out}(t)e^{-i\omega_L t+i\chi_L}+\hat{a}_{\rm out}(t)e^{i\omega_L t-i\chi_L}] , \tag{5.2}$$

where

$$\chi_L=\varphi_L+\tfrac{1}{2}\pi . \tag{5.3}$$

The homodyne signal may then be written as

$$S_{H_{\rm out}}=2\eta f_L^{1/2}\int_0^T dt\langle\hat{X}_{\rm out}(\chi_L,t)\rangle , \tag{5.4}$$

where the detectors of quantum efficiency $\eta$ are activated over the period 0 to $T$.

The noise in the homodyne detection is obtained from the analogous second-order calculation for the case where the detected light is a superposition of the amplifier output and the local oscillator beam. The terms linear in $f_L$ are

$$N_{H_{\rm out}}=\eta(1-\eta)Tf_L+4\eta^2Tf_L\langle[\Delta X_{\rm out}(\chi_L)]^2\rangle , \tag{5.5}$$

where the quadrature operator variance is defined by

$$\langle[\Delta X_{\rm out}(\chi_L)]^2\rangle = \frac{1}{T}\int_0^T dt\int_0^T dt'\langle\hat{X}_{\rm out}(\chi_L,t),\hat{X}_{\rm out}(\chi_L,t')\rangle , \tag{5.6}$$

and we have employed the operator notation

$$\langle\hat{A},\hat{B}\rangle=\langle\hat{A}\hat{B}\rangle-\langle\hat{A}\rangle\langle\hat{B}\rangle . \tag{5.7}$$

For measurements on the input field the expressions for homodyne noise and signal have "out" replaced by "in." They can in principle be evaluated for the different types of input light. We shall be concerned with time-stationary light where a change of variables analogous to Eq. (3.33) enables one of the integrations in Eq. (5.6) to be performed, with the result

$$\langle[\Delta X_{\rm out}(\chi_L)]^2\rangle = \frac{1}{T}\int_{-T}^T dt(T-t)\langle\hat{X}_{\rm out}(\chi_L,t),\hat{X}_{\rm out}(\chi_L,0)\rangle . \tag{5.8}$$

If the correlation function in the integrand is a symmetrical function of $t$, the result reduces to

$$\langle[\Delta X_{\rm out}(\chi_L)]^2\rangle=\int_{-T}^T dt\langle\hat{X}_{\rm out}(\chi_L,t),\hat{X}_{\rm out}(\chi_L,0)\rangle , \tag{5.9}$$

and whether or not this condition is satisfied, an integration time $T$ much longer than the coherence time of the amplifier output reduces the quadrature variance to

$$\langle[\Delta X_{\rm out}(\chi_L)]^2\rangle=\int_{-\infty}^{\infty} dt\langle\hat{X}_{\rm out}(\chi_L,t),\hat{X}_{\rm out}(\chi_L,0)\rangle . \tag{5.10}$$

This result can be evaluated to give a more explicit relation between the output and input variances. Thus the output quadrature operator (5.2) can be related to its input counterpart defined in terms of $\hat{b}^{\dagger}_{\rm in}(t)$ and $\hat{b}_{\rm in}(t)$ with the use of Eq. (2.18). The resulting integrations can be performed, and when the local oscillator and cavity are of the same frequency ($\omega_L=\omega_0$), and the $\hat{a}_{\rm in}$ modes are unexcited, then

$$\langle[\Delta X_{\rm out}(\chi_L)]^2\rangle-\tfrac{1}{4}=\frac{f_{\rm ch}}{\Gamma}+G_0\{\langle[\Delta X_{\rm in}(\chi_L)]^2\rangle-\tfrac{1}{4}\} , \tag{5.11}$$

where $\langle[\Delta X_{\rm in}(\chi_L)]^2\rangle$ is the input quadrature variance analogous to that in Eq. (5.10). The corresponding relation between input and output homodyne noises, for $\omega_L=\omega_0$, can be obtained from Eq. (5.5). In the limit of long integration times this is

$$N_{H_{\rm out}}-\eta Tf_L=\frac{4\eta^2Tf_Lf_{\rm ch}}{\Gamma}+G_0(N_{H_{\rm in}}-\eta Tf_L) . \tag{5.12}$$

We now apply these results to specific inputs.

#### 1. Coherent input

As before in Eqs. (3.36) and (3.39), we assume a quasi-single-mode coherent input and we take the mode frequency to be the local oscillator frequency, $\omega_c=\omega_L$. Consider first the homodyne detection of the input before amplification. From Eq. (5.4), with "out" replaced by "in," we find the input signal to be

$$S_{H_{\rm in}}=2\eta Tf_L^{1/2}f_{\rm in}^{1/2}\sin(\varphi-\varphi_L) , \tag{5.13}$$

which is that obtained by Collett, Loudon, and Gardiner.[20] The input quadrature variance, defined similarly to that for the output in Eq. (5.6), is

$$\langle[\Delta X_{\rm in}(\chi_L)]^2\rangle=\tfrac{1}{4} , \tag{5.14}$$

the standard result for a coherent input, and the noise, from Eq. (5.5), is

$$N_{H_{\rm in}}=\eta Tf_L . \tag{5.15}$$

We therefore find the signal-to-noise ratio of the incoming field to be[20]

$$\left[\frac{S^2}{N}\right]_{H_{\text{in}}} = 4\eta T f_{\text{in}} \sin^2(\varphi - \varphi_L) \ . \tag{5.16}$$

Now consider homodyne detection of the output field. In the $\hat{a}_{\text{in}}$ modes are unexcited then from Eq. (2.18) the operator describing the output has the expectation value

$$\langle \hat{a}_{\text{out}}(t) \rangle = (\gamma_1\gamma_2)^{1/2} \int_{-\infty}^{t} d\tau\, e^{-(i\omega_0+\Gamma)(t-\tau)} \langle \hat{b}_{\text{in}}(\tau) \rangle \ . \tag{5.17}$$

Using Eqs. (3.36) and (3.39) for the coherent input, we find

$$\langle \hat{a}_{\text{out}}(t) \rangle = \frac{(\gamma_1\gamma_2 f_{\text{in}})^{1/2}}{[\Gamma - i(\omega_c - \omega_0)]} e^{-i\omega_c t + i\varphi} \ . \tag{5.18}$$

One effect of the amplifier-cavity system is clearly to introduce a phase shift $\varphi_A$, defined by

$$\frac{1}{[\Gamma - i(\omega_c - \omega_0)]} = \frac{e^{i\varphi_A}}{[\Gamma^2 + (\omega_c - \omega_0)^2]^{1/2}} \ . \tag{5.19}$$

We can write then for Eq. (5.18),

$$\langle \hat{a}_{\text{out}}(t) \rangle = [G(\omega_c) f_{\text{in}}]^{1/2} e^{-i\omega_c t + i\varphi + i\varphi_A} \ . \tag{5.20}$$

Using Eq. (5.4), the output signal thus becomes

$$S_{H_{\text{out}}} = 2\eta T [f_L G(\omega_c) f_{\text{in}}]^{1/2} \sin(\varphi + \varphi_A - \varphi_L) \ , \tag{5.21}$$

where Eqs. (5.2) and (5.3) have also been used. Comparing this to the input signal, given in Eq. (5.13), we see that the effects of amplification are the multiplication of the input by the square root of the gain, and phase shift in $\varphi$ to $\varphi + \varphi_A$.

The noise on the output is found from the results (5.5) and (5.2), and we may use the time-stationary form (5.8) in this case. The quadrature operator has the second-order expectation value, from Eqs. (2.18), (2.19), and (5.2),

$$\langle \hat{X}_{\text{out}}(\chi_L, t), \hat{X}_{\text{out}}(\chi_L, 0) \rangle = \tfrac{1}{2} f_{\text{ch}} e^{-\Gamma|t|} \cos(\omega_c - \omega_0)t + \tfrac{1}{4}\delta(t) \ , \tag{5.22}$$

which is a symmetrical function of $t$ so that we can use Eq. (5.9), and find

$$\langle [\Delta X_{\text{out}}(\chi_L)]^2 \rangle = \tfrac{1}{4} + f_{\text{ch}} \frac{e^{-\Gamma T}\{(\omega_c - \omega_0)\sin[(\omega_c - \omega_0)T] - \Gamma \cos[(\omega_c - \omega_0)T]\} + \Gamma}{(\omega_c - \omega_0)^2 + \Gamma^2} \ . \tag{5.23}$$

We note that the input and output variances, (5.14) and (5.23), respectively, correctly satisfy Eq. (5.11) in the limit $\Gamma T \gg 1$, for $\omega_c = \omega_0$. The output noise is now

$$N_{H_{\text{out}}} = \eta T f_L + 4\eta^2 T f_L f_{\text{ch}} \frac{e^{-\Gamma T}\{(\omega_c - \omega_0)\sin[(\omega_c - \omega_0)T] - \Gamma \cos[(\omega_c - \omega_0)T]\} + \Gamma}{(\omega_c - \omega_0)^2 + \Gamma^2} \tag{5.24}$$

If the local oscillator and cavity are resonant, $\omega_c = \omega_0$, the result reduces to

$$N_{H_{\text{out}}} = \eta T f_L + 4\eta^2 T f_L f_{\text{ch}} \frac{(1 - e^{-\Gamma T})}{\Gamma} \ , \tag{5.25}$$

which is the input noise plus the additional noise due to the amplifier. [Removing the amplifier, $f_{\text{ch}} = 0$, recovers the result (5.15) describing the input.] Taking only the resonant case, we find the signal-to-noise ratio of the output to be given by Eqs. (5.21) and (5.25) as

$$\left[\frac{S^2}{N}\right]_{H_{\text{out}}} = \frac{4\eta T f_{\text{in}} G_0 \sin^2(\varphi + \varphi_A - \varphi_L)}{1 + 2\eta[2\pi f_{\text{ch}}(\omega_0)](1 - e^{-\Gamma T})} \ , \tag{5.26}$$

where $f_{\text{ch}}(\omega_0)$ is defined in Eq. (3.6). In the limit of long integration times this result agrees with the known form[20] of the signal-to-noise ratio for homodyne detection of a superposition of chaotic and coherent light, with the quantity $2\pi f_{\text{ch}}(\omega_0)$ being the resonant chaotic flux in quanta per unit time per unit frequency bandwidth.

If the phase angle $\varphi_L$ is adjusted to maximize the signals, the ratio of the signal-to-noise ratios of input and output (that is, before and after amplification), is

$$R \equiv \frac{(S^2/N)_{H_{\text{out}}}}{(S^2/N)_{H_{\text{in}}}} = \frac{G_0}{1 + 2\eta[2\pi f_{\text{ch}}(\omega_0)](1 - e^{-\Gamma T})} \ . \tag{5.27}$$

Substituting from Eq. (3.25) the value of $f_{\text{ch}}(\omega_0)$ for the optimized asymmetric cavity, the maximum value of $R$ is

$$R_{\max} = \frac{G_0}{1 + 2\eta(G_0 - 1)(1 - e^{-\Gamma T})} \ . \tag{5.28}$$

With a perfect detector ($\eta = 1$), long integration time ($\Gamma T \gg 1$), and a high-gain amplifier ($G_0 \gg 1$), we find that the maximum enhancement is equal to $\frac{1}{2}$, i.e., signal enhancement is impossible. This is similar to the discrete-mode amplifier result,[5] and is not surprising since a very narrow-band input has been assumed here.

More generally, however, it is seen from Eq. (5.28) that signal enhancement is possible ($R > 1$) when

$$2\eta(1 - e^{-\Gamma T}) < 1 \ , \tag{5.29}$$

a result *independent* of the amplifier gain $G_0$. Thus, for a perfect detector amplified homodyne detection appears to

offer an improvement for $T \leq 0.7\Gamma^{-1}$. This condition requires that the detection bandwidth be greater than the amplifier bandwidth. Equivalently, the detector integration time is roughly less than the amplifier storage time, and, as discussed in Ref. 8, this is an improvement attainable *without* amplification, simply by counting over a longer time $T$. In practice, therefore, this is not a useful limit.

For inefficient detectors ($\eta < 1$), and with long integration times, the situation is somewhat different. Figure 4 shows the dependence of signal-to-noise ratio upon detector efficiency $\eta$ for the input (that is, homodyne detection *without* amplification) and the output separately, according to Eqs. (5.16) and (5.26), with phase angles adjusted to optimize signal-to-noise ratio. It is seen that a signal-to-noise ratio improvement is possible when the detector efficiency is less than $\frac{1}{2}$, a result which holds regardless of the amplifier gain $G_0$. In particular, for very low efficiency detectors ($\eta \ll 1$), the enhancement $R$ offered by amplification can approach a value equal to the gain $G_0$. It is clear, however, that, whether or not the signal is amplified, the best signal-to-noise ratio is obtained from the detector of highest quantum efficiency available.

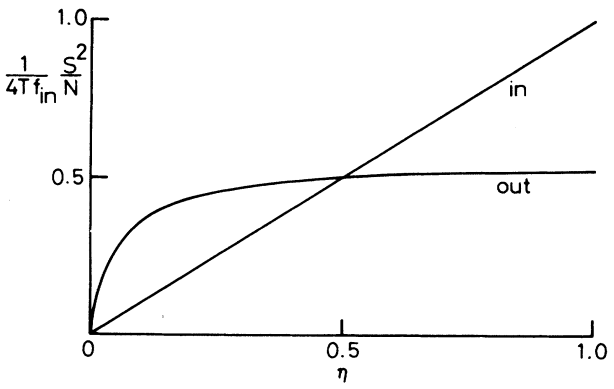


FIG. 4. Dependence of signal-to-noise ratios on detector efficiency $\eta$ for homodyne detection of coherent input light before and after amplification, with $G_0 = 10$ and a long integration time.

### 2. *Chaotic input*

For a chaotic input both incoming and outgoing signals vanish,

$$S_{H_{\text{in}}} = S_{H_{\text{out}}} = 0 \ . \tag{5.30}$$

We assume in calculating the noise that the central frequency of the chaotic input $\omega_c$, the cavity mode frequency $\omega_0$, and the local oscillator frequency $\omega_L$ are all equal. Using Eq. (3.48) for the input correlation then gives

$$\langle \hat{X}_{\text{in}}(\chi_L, t), \hat{X}_{\text{in}}(\chi_L, 0) \rangle = \tfrac{1}{2} f_{\text{in}} e^{-\gamma_c |t|} + \tfrac{1}{4}\delta(t) \tag{5.31}$$

so that the quadrature variance from Eq. (5.9) is

$$\langle [\Delta X_{\text{in}}(\chi_L)]^2 \rangle = \tfrac{1}{4} + f_{\text{in}} \frac{(1 - e^{-\gamma_c T})}{\gamma_c} \ . \tag{5.32}$$

The input noise can now be obtained from Eq. (5.5),

$$N_{H_{\text{in}}} = \eta T f_L + 4\eta^2 T f_L f_{\text{in}} \frac{(1 - e^{-\gamma_c T})}{\gamma_c} \ , \tag{5.33}$$

which is of identical form with Eq. (5.25) describing the *output* noise when the input is coherent. Here the chaotic *input* takes the place of the amplifier-added noise. The output noise for a chaotic input can be calculated, using the correlation function (3.49), to be

$$N_{H_{\text{out}}} = \eta T f_L + 4\eta^2 T f_L \left[ f_{\text{ch}} \frac{1 - e^{-\Gamma T}}{\Gamma} + \frac{\gamma_1 \gamma_2 f_{\text{in}}}{\Gamma(\Gamma^2 - \gamma_c^2)} \left[ \frac{\Gamma}{\gamma_c}(1 - e^{-\gamma_c T}) - \frac{\gamma_c}{\Gamma}(1 - e^{-\Gamma T}) \right] \right] \ . \tag{5.34}$$

Simplifying these results for the limit of long integration times ($\gamma_c T, \Gamma T \gg 1$) produces

$$N_{H_{\text{in}}} = \eta T f_L + 4\eta^2 T f_L f_{\text{in}} / \gamma_c \ , \tag{5.35}$$

$$N_{H_{\text{out}}} = \eta T f_L + 4\eta^2 T f_L \left[ \frac{f_{\text{ch}}}{\Gamma} + \frac{G_0 f_{\text{in}}}{\gamma_c} \right] , \tag{5.36}$$

which conforms to the general relation (5.12).

### 3. *Squeezed input*

As a final example of the application of homodyne detection techniques to assessing the output from our amplifier system, we consider a squeezed input. The incoming beam is said to be squeezed if there are phase angles $\chi_L$ for which[21]

$$\langle [\Delta X_{\text{in}}(\chi_L)]^2 \rangle < \tfrac{1}{4} \ . \tag{5.37}$$

Similarly, the light remains squeezed after processing if

$$\langle [\Delta X_{\text{out}}(\chi_L)]^2 \rangle < \tfrac{1}{4} \ . \tag{5.38}$$

Using the relation (5.11) these conditions may be recast as the requirement that

$$\pi f_{\text{ch}}(\omega_0) + G_0 \{ \langle [\Delta X_{\text{in}}(\chi_L)]^2 \rangle - \tfrac{1}{4} \} < 0 \ . \tag{5.39}$$

For the noise flux $f_{\text{ch}}(\omega_0)$ taking the minimum value in Eq. (3.25) this requires that the resonant gain $G_0$ have an upper bound,

$$G_0 < \frac{2}{1+4\langle[\Delta X_{\text{in}}(\chi_L)]^2\rangle} . \tag{5.40}$$

This is equivalent to the discrete-mode result, and shows the same maximum gain of 2 (Refs. 4 and 5) for a heavily squeezed input with negligible quadrature variance.

### B. Direct detection

For a photodetector of quantum efficiency $\eta$ that receives the output from the amplifier during the period 0 to $T$, the mean photocount is[20]

$$\langle m(T)\rangle_{\text{out}} = \eta\int_0^T dt\,\langle \hat{a}^\dagger_{\text{out}}(t)\hat{a}_{\text{out}}(t)\rangle = \eta\int_0^T dt\, f_{\text{out}}(t) . \tag{5.41}$$

For light of nonstationary statistical properties it is convenient to randomize the counting period start time with respect to any periodicity in the light beam. For light with time-stationary properties, we have, from Eqs. (3.28)–(3.30),

$$\langle m(T)\rangle_{\text{out}} = \eta T f_{\text{out}} . \tag{5.42}$$

The photocount second-factorial moment is[20]

$$\langle m(T)[m(T)-1]\rangle_{\text{out}} = \eta^2\int_0^T dt\int_0^T dt'\langle \hat{a}^\dagger_{\text{out}}(t')\hat{a}^\dagger_{\text{out}}(t)\hat{a}_{\text{out}}(t)\hat{a}_{\text{out}}(t')\rangle . \tag{5.43}$$

The normalized second-factorial moment of the photocount distribution provides a measure of the degree of second-order coherence of the amplifier output field. We accordingly define this to be

$$g^{(2)}_{D_{\text{out}}}(T) = \frac{\langle m(T)[m(T)-1]\rangle_{\text{out}}}{\langle m(T)\rangle^2_{\text{out}}} . \tag{5.44}$$

The photocount variance is given by Eqs. (5.41) and (5.43) as

$$\langle[\Delta m(T)]^2\rangle_{\text{out}} = (1-\eta)\langle m(T)\rangle_{\text{out}} + \eta^2\int_0^T dt\int_0^T dt'\langle \hat{a}^\dagger_{\text{out}}(t)\hat{a}_{\text{out}}(t),\hat{a}^\dagger_{\text{out}}(t')\hat{a}_{\text{out}}(t')\rangle , \tag{5.45}$$

using the shorthand notation defined in Eq. (5.7). The departure of the detected photocount statistics from Poisson form is measured by the Mandel parameter[4]

$$Q_{D_{\text{out}}}(T) = \frac{\langle[\Delta m(T)]^2\rangle_{\text{out}} - \langle m(T)\rangle_{\text{out}}}{\langle m(T)\rangle_{\text{out}}} . \tag{5.46}$$

Expressions analogous to all of the above can be defined for the input light, in the absence of the amplifier and cavity, when the modes $\hat{b}_{\text{in}}(\omega)$ interact directly with the detector: corresponding quantities are denoted by the subscript "in."

### C. Specific inputs

#### 1. Coherent input

If the input field is coherent in the sense defined by Eqs. (3.35) and (3.36) then its mean photocount, given by Eq. (5.41), is taken to be the direct detection signal

$$S_{D_{\text{in}}} = \langle m(T)\rangle_{\text{in}} = \eta T f_{\text{in}} . \tag{5.47}$$

The second-factorial moment (5.43) is

$$\langle m(T)[m(T)-1]\rangle_{\text{in}} = \eta^2 T^2 f^2_{\text{in}} \tag{5.48}$$

so that we find, from Eq. (5.44), a second-order coherence

$$g^{(2)}_{D_{\text{in}}}(T) = 1 , \tag{5.49}$$

characteristic of Poissonian photocount statistics. The direct detection noise is defined to be

$$N_{D_{\text{in}}} = \langle[\Delta m(T)]^2\rangle_{\text{in}} = \eta T f_{\text{in}} . \tag{5.50}$$

The input signal-to-noise ratio is therefore

$$\left[\frac{S^2}{N}\right]_{D_{\text{in}}} = \eta T f_{\text{in}} . \tag{5.51}$$

If we consider now the processed field, direct detection of the amplifier output yields a mean photocount

$$\langle m(T)\rangle_{\text{out}} = \eta T f_{\text{out}} = \eta T(f_{\text{ch}} + G_0 f_{\text{in}}) \tag{5.52}$$

for a resonant input. The output signal for direct detection is defined to be the additional photocount produced by the input,

$$S_{D_{\text{out}}} = \eta T G_0 f_{\text{in}} . \tag{5.53}$$

This is simply the gain times the input signal (5.47). The output second-factorial moment is found from Eq. (5.43) with the second-order correlation (4.4), and it is

$$\langle m(T)[m(T)-1]\rangle_{\text{out}} = \langle m(T)\rangle^2_{\text{out}} + \eta^2\left[\frac{Tf_{\text{ch}}}{\Gamma}\right][f_{\text{ch}}F(2\Gamma T) + 4G_0 f_{\text{in}}F(\Gamma T)] , \tag{5.54}$$

where the function $F(x)$ is defined by

$$F(x) = (e^{-x} - 1 + x)/x , \tag{5.55}$$

having the limiting values

$$F(x)\approx\tfrac{1}{2}x \quad \text{for } x\ll 1 , \tag{5.56}$$

$$F(x)\simeq 1 \quad \text{for } x\gg 1 . \tag{5.57}$$

As we would expect, the degree of second-order coherence (5.44) of the output is greater than unity, tending towards 2 as the amplifier noise dominates the signal. The $Q$ parameter (5.46) is thus larger than zero, showing that the processed field is bunched, with super-Poissonian statistics associated with the chaotic component in the amplifier output.

The signal-to-noise ratio is given by

$$\left[\frac{S^2}{N}\right]_{D_{\text{out}}}=\frac{\eta T G_0^2 f_{\text{in}}^2}{f_{\text{ch}}+G_0 f_{\text{in}}+\eta(f_{\text{ch}}/\Gamma)[f_{\text{ch}}F(2\Gamma T)+4G_0 f_{\text{in}}F(\Gamma T)]} . \tag{5.58}$$

We find the enhancement factor $R$, the ratio of output to input signal-to-noise ratios, from Eqs. (5.51) and (5.58),

$$R_D=\frac{(S^2/N)_{D_{\text{out}}}}{(S^2/N)_{D_{\text{in}}}}=\frac{G_0^2 f_{\text{in}}}{f_{\text{ch}}+G_0 f_{\text{in}}+\eta(f_{\text{ch}}/\Gamma)[f_{\text{ch}}F(2\Gamma T)+4G_0 f_{\text{in}}F(\Gamma T)]} . \tag{5.59}$$

A similar factor has been discussed in detail elsewhere.[8] We note here only its behavior in the case of an intense coherent input, where $G_0 f_{\text{in}}\gg f_{\text{ch}}$. When the cavity asymmetry is optimized according to the discussion in Sec. III, so that the additive noise component $f_{\text{ch}}$ takes the value $(\Gamma/2)(G_0-1)$, as specified in Eq. (3.25), the ratio $R_D$ reduces to

$$R_D=\frac{G_0}{1+2\eta(G_0-1)F(\Gamma T)} . \tag{5.60}$$

Signal enhancement ($R_D>1$) will then be possible if

$$2\eta F(\Gamma T)<1 . \tag{5.61}$$

Note the similarity of Eqs. (5.60) and (5.61) to Eqs. (5.28) and (5.29). Since the functions $(1-e^{-\Gamma T})$ and $F(\Gamma T)$ have a similar behavior over the range of positive $T$, the remarks made about signal enhancement upon amplified homodyne detection also hold for amplified direct detection in the high input intensity limit. In particular, amplification may aid direct detection when only a detector of low quantum efficiency is available.

### 2. *Chaotic input*

In direct detection, unlike the homodyne result (5.30), a chaotic input gives rise to a nonzero signal,

$$S_{D_{\text{in}}}=\langle m(T)\rangle_{\text{in}}=\eta T f_{\text{in}} \tag{5.62}$$

from Eq. (5.41). The second-factorial moment of the photocount is obtained from Eqs. (4.6) and (5.43) as

$$\langle m(T)[m(T)-1]\rangle_{\text{in}}=\eta^2 f_{\text{in}}^2\left[T^2+\frac{T}{\gamma_c}F(2\gamma_c T)\right] . \tag{5.63}$$

This gives

$$g^{(2)}_{D_{\text{in}}}(T)=1+\frac{1}{\gamma_c T}F(2\gamma_c T) \tag{5.64}$$

and the $Q$ parameter (5.46),

$$Q_{D_{\text{in}}}(T)=\frac{\eta f_{\text{in}}}{\gamma_c}F(2\gamma_c T) . \tag{5.65}$$

Given the limiting value (5.56) of $F(2\gamma_c T)$, $g^{(2)}(T)$ is approximately equal to 2 for small $\gamma_c T$. The input signal-to-noise ratio is

$$\left[\frac{S^2}{N}\right]_{D_{\text{in}}}=\frac{\eta T f_{\text{in}}}{1+\eta(f_{\text{in}}/\gamma_c)F(2\gamma_c T)} . \tag{5.66}$$

We turn now to the output. The mean photocount for the processed signal is

$$\langle m(T)\rangle_{\text{out}}=\eta T f_{\text{out}} , \tag{5.67}$$

with $f_{\text{out}}$ given in Eq. (3.50). The additional photocount produced by the input thus gives the output signal

$$S_{D_{\text{out}}}=\eta T\frac{f_{\text{in}}\gamma_1\gamma_2}{\Gamma(\Gamma+\gamma_c)} \tag{5.68}$$

which, as with the coherent result (5.53), is essentially the gain times the input signal. The output second-factorial moment, from Eqs. (5.43) and (4.8), can be written as

$$\begin{aligned}\langle m(T)[m(T-1)]\rangle_{\text{out}}=\langle m(T)\rangle_{\text{out}}^2&+\frac{\eta^2 T}{\Gamma}\left[f_{\text{ch}}-\frac{\gamma_1\gamma_2\gamma_c}{\Gamma(\Gamma^2-\gamma_c^2)}f_{\text{in}}\right]^2 F(2\Gamma T)\\&+\frac{4\eta^2\gamma_1\gamma_2 T}{(\Gamma+\gamma_c)(\Gamma^2-\gamma_c^2)}\left[f_{\text{ch}}-\frac{\gamma_1\gamma_2\gamma_c}{\Gamma(\Gamma^2-\gamma_c^2)}f_{\text{in}}\right]f_{\text{in}}F((\Gamma+\gamma_c)T)\\&+\frac{\eta^2\gamma_1^2\gamma_2^2 T}{\gamma_c(\Gamma^2-\gamma_c^2)^2}f_{\text{in}}^2F(2\gamma_c T) .\end{aligned} \tag{5.69}$$

This expression simplifies in the limit of a short integration time, $\gamma_c T$ and $\Gamma T \ll 1$, where the limit (5.56) applies, and Eq. (5.69) reduces to

$$\langle m(T)[m(T)-1]\rangle_{\text{out}} = 2\langle m(T)\rangle_{\text{out}}^2 . \tag{5.70}$$

The measured degree of second-order coherence defined in Eq. (5.44) is therefore

$$g_{D_{\text{out}}}^{(2)} = 2, \quad \gamma_c T, \Gamma T \ll 1 \tag{5.71}$$

which may be compared with Eq. (4.10). At the opposite limit, for a long integration time, where Eq. (5.57) applies, Eq. (5.69) reduces to

$$\langle m(T)[m(T)-1]\rangle_{\text{out}} = \langle m(T)\rangle_{\text{out}}^2 + \frac{\eta^2 T}{\Gamma+\gamma_c}\left[\left[f_{\text{ch}} + \frac{\gamma_1\gamma_2}{\Gamma(\Gamma+\gamma_c)} f_{\text{in}}\right]^2 + \frac{\gamma_c}{\Gamma}\left[f_{\text{ch}} + \frac{\gamma_1\gamma_2}{\Gamma\gamma_c} f_{\text{in}}\right]^2\right] ,$$

$$\gamma_c T, \Gamma T \gg 1 . \tag{5.72}$$

### 3. *Number-state input*

If we consider the antibunched field described earlier by Eqs. (3.53)–(3.57), then Eq. (5.41) gives the mean detected count to be

$$[\langle m(T)\rangle_{\text{in}}]_{\text{av}} = \eta T (f_{\text{in}})_{\text{av}} = \eta \frac{T}{t_0} , \tag{5.73}$$

where we have used Eq. (3.63) for the input flux.

The second-factorial moment of the input is obtained using Eq. (4.12) as

$$[\langle m(T)[m(T)-1]\rangle_{\text{in}}]_{\text{av}} = \eta^2 \left[\frac{T}{t_0}\left[\frac{T}{t_0}-1\right] + \left[1-\frac{\Delta}{t_0}\right]\frac{\Delta}{t_0}\right] , \tag{5.74}$$

where we have defined

$$T = N t_0 + \Delta, \quad 0 \le \Delta < t_0 , \tag{5.75}$$

that is, the length of time for which the detector is switched on is decomposed into an integral number $N$ of periods of length $t_0$ and a small quantity $\Delta$. Observe that there is zero correlation in the photon stream unless $T > t_0$.

The measured second-order coherence of the input field is then found from Eq. (5.44) to be

$$g_{D_{\text{in}}}^{(2)}(T) = \frac{(T/t_0)[(T/t_0)-1] + [1-(\Delta/t_0)](\Delta/t_0)}{(T/t_0)^2} , \tag{5.76}$$

which is clearly always less than unity and is zero if $T = \Delta$ (i.e., $N=0$). This function is drawn in Fig. 5 and describes a field with sub-Poissonian statistics. The direct detection noise is

$$N_{D_{\text{in}}} = \{\langle [\Delta m(T)]^2\rangle_{\text{in}}\}_{\text{av}} = \eta(1-\eta)(T/t_0) + \eta^2[1-(\Delta/t_0)](\Delta/t_0) , \tag{5.77}$$

which vanishes for a perfectly efficient detector when the integration time $T$ is an integral number of periods $t_0$. The corresponding signal-to-noise ratio is

$$\left[\frac{S^2}{N}\right]_{D_{\text{in}}} = \frac{\eta T^2}{(1-\eta)T t_0 + \eta\Delta(t_0-\Delta)} . \tag{5.78}$$

We now turn to the output field. Direct detection of the amplifier output (3.65) yields a mean photocount

$$[\langle m(T)\rangle_{\text{out}}]_{\text{av}} = \eta f_{\text{ch}} T + \frac{\eta\gamma_1\gamma_2}{\Gamma(\Gamma+\gamma)}(f_{\text{in}})_{\text{av}} T \tag{5.79}$$

for a resonant input. The output signal is then

$$S_{D_{\text{out}}} = \eta T \frac{\gamma_1\gamma_2}{\Gamma(\Gamma+\gamma)}(f_{\text{in}})_{\text{av}} \tag{5.80}$$

or, for a cavity bandwidth much greater than the input signal bandwidth ($\Gamma \gg \gamma$),

$$S_{D_{\text{out}}} = \eta T G_0 (f_{\text{in}})_{\text{av}} \tag{5.81}$$

[cf. Eq. (5.35)]. The output second-factorial moment is, using Eq. (5.43) with the correlation (4.16),

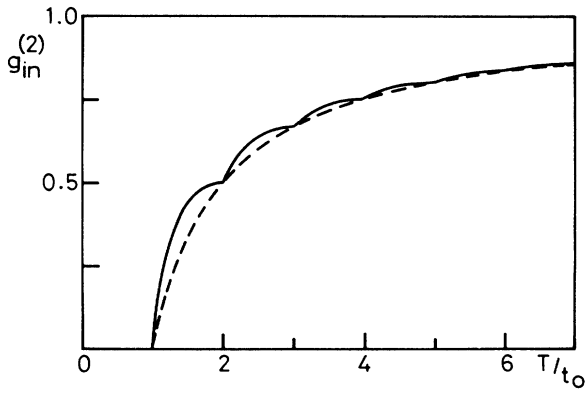


FIG. 5. Solid curve: direct-detection degree of second-order coherence of the photon-number input light. Dashed curve: the function $1-(t_0/T)$ to which the degree of coherence tends for large $T/t_0$.

$$\{\langle m(T)[m(T)-1]\rangle_{\text{out}}\}_{\text{av}}=\eta^2\Bigg\{f_{\text{ch}}^2T^2+f_{\text{ch}}^2(T/\Gamma)F(2\Gamma t) + \frac{2\gamma_1\gamma_2}{\Gamma(\Gamma+\gamma)}\frac{f_{\text{ch}}}{t_0}\left[T^2+\frac{T}{\Gamma-\gamma}\left[\frac{2\Gamma}{\Gamma+\gamma}F((\Gamma+\gamma)T)-\frac{\gamma}{\Gamma}F(2\Gamma T)\right]\right] + \left[\frac{\gamma_1\gamma_2}{\Gamma(\Gamma+\gamma)}\right]^2\left[\frac{T}{t_0}\left[\frac{T}{t_0}-1\right]+\left[1-\frac{\Delta}{t_0}\right]\frac{\Delta}{t_0}\right]\Bigg\}, \tag{5.82}$$

where $F(x)$ is defined in Eqs. (5.55)–(5.57). The direct detection degree of second-order coherence for the amplifier output defined in Eq. (5.44) is obtained by dividing this last expression by the square of Eq. (5.79). It is easily shown that this output coherence is equal to the input coherence (5.76) if $f_{\text{ch}}$ is set equal to zero, but the unavoidable presence of this chaotic amplifier emission increases the output fluctuations above their input value.

The noise introduced by the detection process is minimized by the choice of a very short integration time $T$ such that $(\Gamma+\gamma)T\ll 1$, when $T$ can be set equal to $\Delta$. It follows from Eqs. (5.44), (5.79), and (5.82), with use of the limit (5.56), that in this case

$$g^{(2)}_{D_{\text{out}}}(T)=g^{(2)}_{\text{out}}(0),\quad (\Gamma+\gamma)T\ll 1\ , \tag{5.83}$$

where the form of the degree of second-order coherence $g^{(2)}_{\text{out}}(0)$ is given in Eq. (4.19). The discussion that follows the latter equation thus applies to the direct detection photocount statistics, and, in particular, the maximum amplifier gain for which these statistics show antibunching is given by Eq. (4.22).

## VI. DENSITY-MATRIX EVOLUTION AND INPUT-OUTPUT CHARACTERISTIC FUNCTIONS

The treatment of the system thus far has involved the Heisenberg-picture evolution of input, output, and internal operators. An alternative and concise description of the system evolution is provided by knowledge of the Schrödinger-picture evolution of the appropriate density matrix. We shall now demonstrate that this knowledge is available in the form of certain moment-generating functions and functionals, the determination of which is a prerequisite to the computation of distributions of cavity photons, detected output photoelectrons, and other field-related quantities.

The cavity field density operator $\hat{\rho}(t)$ is related to the appropriate Glauber-Sudarshan $P$ distribution $P(\alpha,\alpha^*;t)$ according to[22]

$$\hat{\rho}(t)=\int d^2\alpha\, P(\alpha,\alpha^*;t)|\alpha\rangle\langle\alpha|\ , \tag{6.1}$$

where $|\alpha\rangle$ is an eigenstate of $\hat{a}(0)$, with eigenvalue $\alpha$. In turn, the Fourier transform of $P(\alpha,\alpha^*;t)$ is given by $\chi_N(\xi,\xi^*;t)$,

$$\chi_N(\xi,\xi^*;t)=\int d^2\alpha\, P(\alpha,\alpha^*;t)e^{\xi\alpha^*-\xi^*\alpha}\ , \tag{6.2}$$

which is the normal-order characteristic function, defined by

$$\chi_N(\xi,\xi^*;t)=\langle\exp[\xi\hat{a}^\dagger(t)]\exp[-\xi^*\hat{a}(t)]\rangle\ , \tag{6.3}$$

and thus $\chi_N(\xi,\xi^*;t)$ gives a complete dynamical description of the cavity mode. This, in turn, is related to the Weyl function $\chi_W(\xi,\xi^*;t)$,

$$\chi_W(\xi,\xi^*;t)=\langle\exp[\xi\hat{a}^\dagger(t)-\xi^*\hat{a}(t)]\rangle\ , \tag{6.4}$$

via the relation

$$\chi_W(\xi,\xi^*;t)=\exp(-\tfrac{1}{2}|\xi|^2)\chi_N(\xi,\xi^*;t)\ , \tag{6.5}$$

which is a consequence of the Baker-Campbell-Hausdorff (BCH) formula.[23]

We may now evaluate $\chi_W$ using a method similar to that of Louisell.[3] The Fourier transform of Eq. (2.12), relating the input and internal fields, is

$$\hat{a}(t)=\gamma_2^{1/2}\int_{-\infty}^{t}d\tau\, e^{-(i\omega_0+\Gamma)(t-\tau)}\hat{b}_{\text{in}}(\tau) +\gamma_1^{1/2}\int_{-\infty}^{t}d\tau\, e^{-(i\omega_0+\Gamma)(t-\tau)}\hat{a}_{\text{in}}(\tau) +\sum_j\frac{k_j\hat{\sigma}_j^-(t_0)e^{-i\omega_j(t-t_0)}}{\omega_j-\omega_0+i\Gamma}\ . \tag{6.6}$$

Substituting Eq. (6.6) into Eq. (6.4), and exploiting the commutativity of the operators $\hat{b}_{\text{in}}$, $\hat{a}_{\text{in}}$, and $\hat{\sigma}_j^-$, we obtain

$$\chi_W(\xi,\xi^*;t)=\chi_W^b\{\xi_b(\tau)\}\chi_W^a\{\xi_a(\tau)\}S(\xi,\xi^*;t)\ , \tag{6.7}$$

where $\chi_W^b\{\xi(\tau)\}$ is the Weyl *functional* of the field $\hat{b}_{\text{in}}(\tau)$, defined by

$$\chi_W^b\{\xi(\tau)\}=\left\langle\exp\left[\int_{-\infty}^{\infty}d\tau\,\xi(\tau)\hat{b}_{\text{in}}^\dagger(\tau) -\int_{-\infty}^{\infty}d\tau\,\xi^*(\tau)\hat{b}_{\text{in}}(\tau)\right]\right\rangle\ , \tag{6.8}$$

and

$$\xi_a(\tau)=\xi\gamma_1^{1/2}\Theta(t-\tau)\exp[(i\omega_0-\Gamma)(t-\tau)]\ , \tag{6.9}$$

$$\xi_b(\tau)=\xi\gamma_2^{1/2}\Theta(t-\tau)\exp[(i\omega_0-\Gamma)(t-\tau)]\ , \tag{6.10}$$

and $S(\xi,\xi^*;t)$ is given by

$$S(\xi,\xi^*;t)=\left\langle\exp\left[\sum_j\frac{\xi k_j\hat{\sigma}_j^+e^{i\omega_j(t-t_0)}}{\omega_j-\omega_0-i\Gamma}-\text{H.c.}\right]\right\rangle \tag{6.11}$$

(where H.c. denotes the Hermitian conjugate). Since the

atoms are considered as independent, we may write $S$ in the form

$$S(\zeta,\zeta^*;t)=\prod_j \left\langle \exp\left[\frac{\zeta k_j \hat{\sigma}_j^{+} e^{i\omega_j(t-t_0)}}{\omega_j-\omega_0-i\Gamma}-\text{H.c.}\right]\right\rangle . \tag{6.12}$$

Use of the identity

$$\exp(x\hat{\sigma}^{\dagger}-y\hat{\sigma}^{-}) =\cos(xy)^{1/2}+\frac{\sin(xy)^{1/2}}{(xy)^{1/2}}(x\hat{\sigma}^{+}-y\hat{\sigma}^{-}) \tag{6.13}$$

and the diagonal nature of each atomic density operator [Eq. (2.9)],

$$\langle \hat{\sigma}_j^{\pm}\rangle=0 \tag{6.14}$$

gives

$$S(\zeta,\zeta^*;t)=\prod_j \cos\left[\frac{|\zeta|k_j}{[(\omega_j-\omega_0)^2+\Gamma^2]^{1/2}}\right] . \tag{6.15}$$

Equation (6.15) may be approximated for small $k_j$ by the replacement

$$\cos\left[\frac{|\zeta|k_j}{[(\omega_j-\omega_0)^2+\Gamma^2]^{1/2}}\right] \simeq \exp\left[-\frac{1}{2}\frac{|\zeta|^2k_j^2}{(\omega_j-\omega_0)^2+\Gamma^2}\right] , \tag{6.16}$$

so that, in the continuum approximation, the resulting summation over atomic terms may be replaced by an integral, giving

$$S(\zeta,\zeta^*;t)\simeq\exp\left[-\tfrac{1}{2}|\zeta|^2\int_{-\infty}^{\infty}\frac{d\omega_j\rho(\omega_j)k^2(\omega_j)}{(\omega_j-\omega_0)^2+\Gamma^2}\right] , \tag{6.17}$$

where $\rho(\omega)$ is the density of states employed earlier. Performing the integral under the conditions assumed in Sec. II, and using Eq. (2.13), we obtain

$$S(\zeta,\zeta^*;t)=\exp\left[-\tfrac{1}{2}|\zeta|^2\frac{n_a\gamma_A}{\Gamma}\right] , \tag{6.18}$$

which represents a Gaussian noise contribution to the internal field statistics. In Appendix A it is shown that the resulting equation connecting the characteristic function of the internal field to the characteristic functionals of the external fields is

$$\chi_N(\zeta,\zeta^*;t)=\exp\left[-|\zeta|^2\frac{n_e\gamma_A}{\Gamma}\right]\chi_N^b\{\xi_b(\tau)\}\chi_N^a\{\xi_a(\tau)\} . \tag{6.19}$$

Equation (6.19) permits either of the input fields $\hat{a}_{\text{in}},\hat{b}_{\text{in}}$ to be in its vacuum state, upon setting the appropriate normal-order functional to unity. Note that in the absence of an input, the internal field characteristic function is a simple Gaussian, and represents a thermal field of mean photon number

$$\bar{n}=\frac{n_e\gamma_A}{\Gamma} . \tag{6.20}$$

If, instead, the inputs are coherent states $|\{\alpha_{\text{in}}(\tau)\}\rangle$ and $|\{\beta_{\text{in}}(\tau)\}\rangle$, specified by the deterministic functions $\alpha_{\text{in}}(\tau)$ and $\beta_{\text{in}}(\tau)$, Eq. (6.19) provides

$$\chi_N(\zeta,\zeta^*;t)=\exp\left[-|\zeta|^2\frac{n_e\gamma_A}{\Gamma}+\zeta f^*(t)-\zeta^* f(t)\right] , \tag{6.21}$$

where

$$f(t)=\int_{-\infty}^{t} d\tau\, e^{-(i\omega_0+\Gamma)(t-\tau)}[\gamma_2^{1/2}\beta_{\text{in}}(\tau)+\gamma_1^{1/2}\alpha_{\text{in}}(\tau)] . \tag{6.22}$$

Using similar methods we may eliminate the internal field to express the characteristic functionals of the output fields in terms of those of the input. Thus, it is shown in Appendix B that

$$\chi_N^{a_{\text{out}}}\{\xi\}=\chi_N^{a_{\text{in}}}\{\xi_a\}\chi_N^{b_{\text{in}}}\{\xi_b\}\exp\left[-\frac{\gamma_1 n_e\gamma_A}{\Gamma}\int_{-\infty}^{\infty}dt_1\int_{-\infty}^{\infty}dt_2\xi^*(t_2)C(t_1-t_2)\xi(t_1)\right] , \tag{6.23}$$

where

$$\xi_a(\tau)=-\xi(\tau)+\gamma_1\int_0^{\infty}dt\,\xi(t+\tau)e^{i(\omega_0+i\Gamma)t} , \tag{6.24}$$

$$\xi_b(\tau)=(\gamma_1\gamma_2)^{1/2}\int_0^{\infty}dt\,\xi(t+\tau)e^{i(\omega_0+i\Gamma)t} , \tag{6.25}$$

and

$$C(\tau)=\exp(-i\omega_0\tau-\Gamma|\tau|) . \tag{6.26}$$

Equation (6.23) enables us to derive input-output relations for any normal-order moment by functionally differentiating $\chi_N^{a_{\text{out}}}\{\xi\}$ with respect to $\xi(t)$ and $\xi^*(t)$ the appropriate number of times. For example, let us assume that the field $\hat{a}_{\text{in}}$ is in its vacuum state ($\chi_N^{a_{\text{in}}}\{\xi_a\}=1$). Then the first-order output coherence function is given by

$$\langle \hat{a}^{\dagger}_{\rm out}(t)\hat{a}_{\rm out}(t')\rangle = -\frac{\delta}{\delta\zeta(t)}\frac{\delta}{\delta\zeta^*(t')}\chi_N^{a_{\rm out}}\{\zeta\}\Big|_{\zeta=\zeta^*=0} . \tag{6.27}$$

Performing the required differentiation in Eq. (6.23), and using the following identities,

$$\frac{\delta}{\delta\xi(t)}\xi_b(\tau)=(\gamma_1\gamma_2)^{1/2}\Theta(t-\tau)e^{i(\omega_0+i\Gamma)(t-\tau)} \tag{6.28}$$

and

$$\frac{\delta^2}{\delta\zeta(t)\delta\zeta^*(t')}\chi^b\{\xi_b\}=\int_{-\infty}^{\infty}\int_{-\infty}^{\infty}dt_1dt_2\frac{\delta\xi_b(t_1)}{\delta\zeta(t)}\frac{\delta\xi_b^*(t_2)}{\delta\zeta^*(t')}\frac{\delta^2\chi^b\{\xi_b\}}{\delta\xi_b(t_1)\delta\xi_b(t_2)} \tag{6.29}$$

gives

$$\langle \hat{a}^{\dagger}_{\rm out}(t)\hat{a}_{\rm out}(t')\rangle=(\gamma_1\gamma_2)\int_{-\infty}^{\infty}\int_{-\infty}^{\infty}dt_1dt_2\langle \hat{b}^{\dagger}_{\rm in}(t_1)\hat{b}_{\rm in}(t_2)\rangle e^{i(\omega_0+i\Gamma)(t-t_1)}e^{i(\omega_0-i\Gamma)(t'-t_2)}\Theta(t'-t_2)+\frac{\gamma_1 n_e\gamma_A}{\Gamma}C(t-t') , \tag{6.30}$$

which is identical to Eq. (3.31).

Higher-order differentiation provides corresponding higher-order time-dependent moments. Thus $\chi_N^a\{\zeta\}$ and $\chi_N^b\{\zeta\}$ contain a complete dynamical description of the system. The output integrated photoelectron distributions, for which we have computed only the first and second moments in Sec. V, require a knowledge of *all* higher-order output field moments, and can be calculated directly from $\chi_N^a\{\zeta\}$. The calculation and study of these distributions will not be given here.

## VII. DISCUSSION AND CONCLUSIONS

We have presented a comprehensive account of the properties of an optical amplifier that consists of an inverted-population atomic medium placed inside a high-$Q$ cavity. The conditions on the system are assumed to be such that only a single mode is significantly excited in the interior of the cavity, but the input and output fields are free-space continuous-mode excitations. In contrast to previous work on amplifiers with single-mode input and output fields, the theory presented here allows the effects of amplification on spectral and temporal correlation functions to be calculated. The amplifier is assumed throughout to be operated in its linear regime, with any response of the atomic level populations to fluctuations in the optical intensity ignored.

Caves[1] has evaluated the limits imposed by quantum theory on the amounts of noise that must be added to the signal in the linear amplification process, and his results for single-mode systems have been extensively illustrated by calculations on specific amplifier models. The continuous-mode theory described in the present paper provides an illustration of Caves's more general limits for the multimode linear amplifier. A noteworthy feature of the cavity amplifier, discussed in Sec. III, is the requirement that the cavity should be asymmetric in order to achieve the minimum noise limit, with the mirror on its output side more highly reflecting than that on its input side. Although the details are different, this requirement is reminiscent of the need for an unsymmetrical cavity in the parametric generation of lowest-noise squeezed light.[10]

Most practical applications of optical amplification use approximately coherent or chaotic input light, and we have given results for the effects of amplification on the optical spectra and on the first- and second-order coherence of these types of light. We have treated both direct and homodyne detection, and have evaluated the relevant signal-to-noise ratios before and after amplification. The possibilities for improving signal-to-noise ratios by amplification of a coherent signal have been investigated.

Nonclassical light beams may in the future be used to carry optical signals, and it is interesting to evaluate the effects of amplification on their low-noise properties. Thus squeezed light can produce less noise than coherent light in a homodyne detector for suitable choices of phase angles, and there has been much speculation on the promise of such light for use in optical communications. Unfortunately, the kind of amplifier treated here tends to destroy the desirable squeezed characteristics of the input light, and we have shown quite generally in Sec. V that even with the most favorable values of the parameters, the output light preserves some squeezing only for gains up to a maximum of 2. Analogous low-noise properties can be achieved in direct detection when the signal light is antibunched. It is more difficult to treat the amplification of antibunched light with the same degree of generality as that of squeezed light, and we have restricted attention to the particular case of the "number-state" input introduced in Sec. III. This state represents an infinite chain of equally spaced pulses, a "photon machine-gun," and it is in many respects the free-space traveling-wave analog of the closed-cavity single-mode state in which a definite number of photons is excited. We have shown indeed in Sec. IV that the maximum gain for which some of the input antibunching is preserved in the output has the same small value for the amplifier treated here as has been found in previous calculations for single-mode systems. The improved theory of the present paper does not therefore generate any greater optimism for the application of inverted-population amplifiers to the processing of signals on nonclassical light beams.

The system considered here, with the amplifying medium confined in a cavity of sufficiently high $Q$ to involve only a single internal mode, is simple enough to enable all the interesting output properties to be evaluated analytically. Thus even the integrated photodetection statistics can be calculated straightforwardly and a basic understanding can be gained of the physical natures of the noise limitations in amplification and detection. However, the presence of the high-$Q$ cavity would be a drawback in many practical applications, where the optical trapping effect of the cavity would produce an unacceptable temporal smearing of the signal. Thus, for example, in high-bit-rate optical communications, it is the practice to coat amplifying media with antireflection films and reduce any cavity effects as much as possible. In future work, therefore, we look to the derivation of a similarly comprehensive theory for a traveling-wave amplifying medium with negligible boundary reflectivities.

## ACKNOWLEDGMENTS

G.L.M. thanks the Science and Engineering Research Council for financial support.

## APPENDIX A

In this appendix we derive the relation between the characteristic functionals of the input fields $\hat{a}_{\rm in}(t),\hat{b}_{\rm in}(t)$, and the characteristic function of the internal field $\hat{a}(t)$.

Beginning with Eq. (6.7), relating to the associated Weyl functions and functionals, the BCH equation[22] is invoked to transform to the associated normal-order characteristic function or functional

$$\chi_W(\zeta,\zeta^*)=e^{-(1/2)|\zeta|^2}\chi_N(\zeta,\zeta^*)\ , \tag{A1}$$

$$\chi_W^a\{\zeta(t)\}=\exp\left[-\tfrac{1}{2}\int_{-\infty}^{\infty}dt\,|\zeta(t)|^2\right]\chi_N^a\{\zeta(t)\}\ , \tag{A2}$$

where

$$\chi_N^a\{\zeta(t)\}=\left\langle\exp\left[\int_{-\infty}^{\infty}\zeta(t)\hat{a}_{\rm in}^{\dagger}(t)dt\right]\right.$$
$$\left.\times\exp\left[-\int_{-\infty}^{\infty}\zeta^*(t)\hat{a}_{\rm in}(t)dt\right]\right\rangle\ . \tag{A3}$$

Note that the BCH equation requires the validity of the requisite canonical commutators, which are valid here for $\hat{a}(t)$ in the linearizing approximation used throughout this paper, and which is implicit in the field-averaging procedure. Thus, from Eq. (6.7), we obtain

$$\chi_N(\zeta,\zeta^*;t)=\exp\left[-\tfrac{1}{2}|\zeta|^{1/2}\left[\frac{n_a\gamma_A}{\Gamma}-1\right]\right]\exp\left[-\tfrac{1}{2}\int_{-\infty}^{\infty}d\tau[|\zeta_b(\tau)|^2+|\zeta_a(\tau)|^2]\right]\chi_N^b[\zeta_b(\tau)]\chi_N^a[\zeta_a(\tau)]\ . \tag{A4}$$

Using Eqs. (6.9) and (6.10) for $\zeta_a$ and $\zeta_b$, we may evaluate the second factor of Eq. (A4),

$$\exp\left[-\tfrac{1}{2}\int_{-\infty}^{\infty}d\tau[|\zeta_b(\tau)|^2+|\zeta_a(\tau)|^2]\right]$$
$$=\exp\left[-\frac{1}{2\Gamma}|\zeta|^2\tfrac{1}{2}(\gamma_1+\gamma_2)\right]\ . \tag{A5}$$

Equation (6.19) is obtained by substituting Eq. (A5) into Eq. (A4), and using Eq. (2.13) for $\Gamma$.

## APPENDIX B

In this appendix we outline the derivation of Eqs. (6.23)–(6.26), relating the output characteristic functional $\chi_N^{\rm out}\{\zeta\}$ to those of the input fields.

The Weyl function for the output field $\hat{a}_{\rm out}(t)$ is defined by

$$\chi_W^{a_{\rm out}}\{\zeta\}=\left\langle\exp\left[\int_{-\infty}^{\infty}d\tau\,\zeta(\tau)\hat{a}_{\rm out}^{\dagger}(\tau)-{\rm H.c.}\right]\right\rangle\ . \tag{B1}$$

Substituting for $\hat{a}_{\rm out}(t)$ from Eq. (2.18), and exploiting the commutativity of the fields $\hat{a}_{\rm in}(t)$, $\sigma_j^+$, and $\hat{b}_{\rm in}(t)$ gives

$$\chi_W^{a_{\rm out}}\{\zeta\}=\chi_W^{a_{\rm in}}\{\xi_a\}\chi_W^{b_{\rm in}}\{\xi_b\}S\{\zeta\}\ , \tag{B2}$$

where $\chi_W^{a_{\rm in}}$ and $\chi_W^{b_{\rm in}}$ are Weyl functionals for the input fields $\hat{a}_{\rm in}(t)$ and $\hat{b}_{\rm in}(t)$, and $\xi_a(t)$ and $\xi_b(t)$ are the functions defined in Eqs. (6.24) and (6.25). $S\{\zeta\}$ is the functional

$$S\{\zeta\}=\left\langle\exp\left[\gamma_1^{1/2}\int_{-\infty}^{\infty}dt\,\zeta(t)\sum_j\frac{k_j\hat{\sigma}_j^{+}e^{i\omega_j(t-t_0)}}{\omega_j-\omega_0+i\Gamma}\right.\right.$$
$$\left.\left.-{\rm H.c.}\right]\right\rangle\ . \tag{B3}$$

We now transform $\zeta(t)$ into the Fourier domain in Eq. (B3), i.e.,

$$\tilde{\zeta}(\omega)=(2\pi)^{-1/2}\int_{-\infty}^{\infty}dt\,\zeta(t)e^{i\omega t}\ , \tag{B4}$$

and employ operator methods similar to those in Eqs. (6.11)–(6.15) to obtain

$$S\{\zeta\}=\prod_j\cos\left[\frac{(2\pi\gamma_1)^{1/2}|\tilde{\zeta}(\omega_j)|k_j}{[(\omega_j-\omega_0)^2+\Gamma^2]^{1/2}}\right]\ . \tag{B5}$$

For small $k_j$ we make the approximation

$$S\{\zeta\}\simeq\exp\left[-\tfrac{1}{2}\sum_j\frac{2\pi|\tilde{\zeta}(\omega_j)|^2k_j^2\gamma_1}{(\omega_j-\omega_0)^2+\Gamma^2}\right]\ . \tag{B6}$$

In the continuum limit, the summation is performed as for Eq. (3.31) to give

$$S\{\zeta\}=\exp\left[-\tfrac{1}{2}\gamma_1\rho(\omega_0)k^2(\omega_0)\frac{\pi}{\Gamma}\int_{-\infty}^{\infty}dt_1\int_{-\infty}^{\infty}dt_2\zeta(t_1)\zeta^*(t_2)e^{-i\omega_0(t_2-t_1)-\Gamma|t_2-t_1|}\right]. \tag{B7}$$

With the use of Eq. (2.13), this becomes

$$S\{\zeta\}=\exp\left[-\tfrac{1}{2}\gamma_1\gamma_A\frac{n_a}{\Gamma}\int_{-\infty}^{\infty}dt_1\int_{-\infty}^{\infty}dt_2\zeta^*(t_2)C(t_2-t_1)\zeta(t_1)\right], \tag{B8}$$

where

$$C(\tau)=\exp(-i\omega_0\tau-\Gamma|\tau|)\ . \tag{B9}$$

The transformation of Weyl functionals to normal-order characteristic functionals is again performed using the BCH theorem, which applies for $\chi_W^{\text{out}}$ and $\chi_N^{\text{out}}$ provided that both $\hat{a}_{\text{in}}$ and $\hat{b}_{\text{in}}$ are retained in the computation to maintain unitarity. Thus

$$\chi_W^{a_{\text{out}}}\{\zeta\}=\exp\left[-\tfrac{1}{2}\int_{-\infty}^{\infty}dt|\zeta(t)|^2\right]\chi_N^{a_{\text{out}}}\{\zeta\}\ . \tag{B10}$$

Applying this to all functionals in Eq. (B2) gives

$$\chi_N^{a_{\text{out}}}\{\zeta\}=\chi_N^{a_{\text{in}}}\{\xi_a\}\chi_N^{b_{\text{in}}}\{\xi_b\}S\{\zeta\}e^{F\{\zeta\}}\ , \tag{B11}$$

where

$$F\{\zeta\}=-\tfrac{1}{2}\int_{-\infty}^{\infty}dt[|\xi_a(t)|^2+|\xi_b(t)|^2-|\zeta(t)|^2]\ . \tag{B12}$$

The integration in Eq. (B12) is carried out after using Eqs. (6.24) and (6.25) for $\xi_a$ and $\xi_b$, and eventually gives

$$F\{\zeta\}=-\tfrac{1}{2}\gamma_1\left[\frac{\gamma_1+\gamma_2}{2\Gamma}-1\right]\int_{-\infty}^{\infty}dt_1\int_{-\infty}^{\infty}dt_2\zeta(t_1)\zeta^*(t_2)C(t_2-t_1)\ . \tag{B13}$$

With the definition of $\Gamma$ in Eq. (2.13), we may then show that

$$S\{\zeta\}e^{F\{\zeta\}}=\exp\left[-\frac{\gamma_1 n_e\gamma_A}{\Gamma}\int_{-\infty}^{\infty}dt_1\int_{-\infty}^{\infty}dt_2\zeta^*(t_2)C(t_2-t_1)\zeta(t_2)\right], \tag{B14}$$

which, in Eq. (B11), completes the derivation of Eq. (6.23).


[1]C. M. Caves, Phys. Rev. D **26**, 1817 (1982).
[2]J. P. Gordon, L. R. Walker, and W. H. Louisell, Phys. Rev. **130**, 806 (1963).
[3]W. H. Louisell, *Radiation and Noise in Quantum Electronics* (McGraw-Hill, New York, 1964), Sec. 7.6.
[4]S. Friberg and L. Mandel, Opt. Commun. **46**, 141 (1983).
[5]R. Loudon and T. J. Shepherd, Opt. Acta **31**, 1243 (1984).
[6]S. Friberg and L. Mandel, in *Coherence in Quantum Optics V,* edited by L. Mandel and E. Wolf (Plenum, New York, 1984), p. 465.
[7]C. K. Hong, S. Friberg, and L. Mandel, J. Opt. Soc. Am. B **2**, 494 (1985).
[8]T. J. Shepherd and E. Jakeman, J. Opt. Soc. Am. B **4**, 1860 (1987).
[9]G. L. Mander, R. Loudon, and T. J. Shepherd, in *Photons and Quantum Fluctuations,* edited by E. R. Pike and H. Walther (Adam Hilger, Bristol, 1988), p. 190.
[10]M. J. Collett and C. W. Gardiner, Phys. Rev. A **30**, 1386 (1984).
[11]Y. Yamamoto and N. Imoto, IEEE J. Quantum Electron. **QE-22**, 2032 (1986).
[12]H. Haken, in *Laser Theory,* Vol. XXV/2c of *Handbuch der Physik,* edited by S. Flügge (Springer, Berlin, 1970).
[13]M. Ley and R. Loudon, J. Mod. Opt. **34**, 227 (1987).
[14]S. M. Barnett and P. M. Radmore, Opt. Commun. **68**, 364 (1988).
[15]R. J. Glauber, in *Frontiers in Quantum Optics,* edited by E. R. Pike and S. Sarkar (Adam Hilger, Bristol, 1986).
[16]For a general discussion see, e.g., S. Stenholm, Phys. Scr. **T12**, 56 (1986).
[17]E. Jakeman, in *Photon Correlation and Light-Beating Spectroscopy,* edited by H. Z. Cummins and E. R. Pike (Plenum, New York, 1974), pp. 75–149.
[18]M. J. Collett (private communication).
[19]R. Loudon, *The Quantum Theory of Light,* 2nd ed. (Oxford University Press, London, 1983).
[20]M. J. Collett, R. Loudon, and C. W. Gardiner, J. Mod. Opt. **34**, 881 (1987).
[21]D. F. Walls, Nature (London) **306**, 141 (1983).
[22]R. J. Glauber, in *Quantum Optics and Electronics,* edited by C. de Witt, A. Blandin, and C. Cohen-Tannoudji (Gordon and Breach, New York, 1965), pp. 65–185.
[23]R. Gilmore, *Lie Groups, Lie Algebras, and Some of Their Applications* (Wiley, New York, 1974).